




Bioprinting: A Strategy to Build Informative Models of Exposure and Disease

Jose Caceres-Alban , Student Member, IEEE, Midori Sanchez , Member, IEEE,
and Fanny L. Casado , Senior Member, IEEE

(Methodological Review)

I. INTRODUCTION

Abstract—Novel additive manufacturing techniques are revolutionizing fields of industry providing more dimensions to control and the versatility of fabricating multi-material products. Medical applications hold great promise to manufacture constructs of mixed biologically compatible materials together with functional cells and tissues. We reviewed technologies and promising developments nurturing innovation of physiologically relevant models to study safety of chemicals that are hard to reproduce in current models, or diseases for which there are no models available. Extrusion-, inkjet- and laser-assisted bioprinting are the most used techniques. Hydrogels as constituents of bioinks and biomaterial inks are the most versatile materials to recreate physiological and pathophysiological microenvironments. The highlighted bioprinted models were chosen because they guarantee post-printing cellular viability while maintaining desirable mechanical properties of their constitutive bioinks or biomaterial inks to ensure their printability. Bioprinting is being readily adopted to overcome ethical concerns of *in vivo* models and improve the automation, reproducibility, geometry stability of traditional *in vitro* models. The challenges for advancing the technological level readiness of bioprinting require overcoming heterogeneity, microstructural complexity, dynamism and integration with other models, to generate multi-organ platforms that can inform about biological responses to chemical exposure, disease development and efficacy of novel therapies.

Index Terms—Disease modeling, additive manufacturing, chemical safety, bioprinting.

Manuscript received 24 July 2021; revised 5 November 2021; accepted 26 December 2021. Date of publication 27 January 2022; date of current version 6 January 2023. The work of Fanny L. Casado was supported by the Project Concytec-Banco Mundial “Mejoramiento y Ampliación de los Servicios del Sistema Nacional de Ciencia, Tecnología e Innovación Tecnológica” under Grant 8682-PE, administered by Prociencia under Contract 052-2018-FONDECYT-BM-IADT-AV. (Corresponding author: Fanny L. Casado.)

Jose Caceres-Alban is with the Institute for Omics Sciences and Applied Biotechnology, Pontificia Universidad Católica del Perú, 15088 San Miguel, Lima, Peru, and also with the Biomedical Engineering Program PUCP-UPCH, Universidad Peruana Cayetano Heredia, 15102 San Martín de Porres, Lima, Peru (e-mail: caceres.jose@pucp.edu.pe).

Midori Sanchez is with the VEO 3D Digital Manufacturing Laboratory, Department of Engineering, Pontificia Universidad Católica del Perú, 15088 San Miguel, Lima, Peru (e-mail: sanchez.ac@pucp.edu.pe).

Fanny L. Casado is with the Institute for Omics Sciences and Applied Biotechnology, Pontificia Universidad Católica del Perú, 15088 San Miguel, Lima, Peru (e-mail: fanny.casado@pucp.edu.pe).

This article has supplementary downloadable material available at <https://doi.org/10.1109/RBME.2022.3146293>, provided by the authors.

Digital Object Identifier 10.1109/RBME.2022.3146293

DURING the pre-clinical stage of drug development, *in vitro* assays serve to (1) obtain safety and toxicity data of a drug candidate, (2) study the mechanisms of action to identify potential adverse effects prior to *in vivo* studies; and (3) are also implemented for personalized medicine applications [1], [2]. Thus, there is an expectation of high-fidelity biomimicry close to modeling physiological and pathophysiological *in vivo* events. *In vitro* bidimensional culture has been practiced since 1907 [3] and it is currently a traditional methodology for toxicological assays due to its affordability, simplicity of fabrication, compatibility with cell imaging systems and the vast number of studies implemented. However, they do not represent an ideal model when compared with three-dimensional (3D) cultures in terms of cell-cell and cell-ECM interactions; gene regulation [4], [5]; morphology [6], [7]; differentiation [8]; access to nutrients, oxygen, drugs or metabolites gradients [9]; and secretion dynamics and signaling components that include proteins and nucleic acids [10], [11]. Manually conducted methods present shortcomings related to spatial control, automation and standardization regardless of being 3D or monolayer cultures. 3D bioprinting is a computer-aided technology that can be implemented in the pharmaceutical and toxicological fields to confer reproducibility, automation, precision and dimensional control to the manufacturing process of bioengineered *in vitro* models when compared to other fabrication methods used to develop disease models such as freeze-drying, electrospinning and spheroid formation.

This article focuses on recent advances in bioprinting to design and validate novel toxicological models of exposure in healthy tissues and safety when testing novel therapies in pathological tissues. We start by introducing the different bioprinting techniques currently available and then, we discuss the characteristics of the most popular bioinks at toxicologist's disposal. Finally, we summarize the state of the art of different tissues and provide a roadmap for their use as *in vitro* models of exposure and disease.

II. BIOPRINTING TECHNIQUES

Biological material deposition strategies date back to the 1980s when a layer of fibronectin was deposited on a plastic surface [12]. Later, during the first decade of the 21st century, the first 3D printed human organ was transplanted [13]; novel inkjet modified printers for proteins and living cells were introduced [14] and first patented; cell spherical aggregates were developed

as an alternative for bioink [15]; and the first commercial bioprinter was invented. These are some of the milestones [16], [17] leading to the field of bioprinting to hold onto its promise to revolutionize health care. While there are excellent reviews of the different bioprinting techniques available, we summarize below the most relevant technologies to create structures of interest for safety analysis of therapeutic products and disease progression. We organized the technologies following the classification for additive manufacturing processes proposed by the American Society for Testing and Materials (ASTM) and the International Organization for Standardization (ISO) [18].

A. Material Extrusion

This process describes technologies in which the material used is selectively dispensed through a nozzle or orifice.

1) Extrusion-based Bioprinting (EBB): This contact technique dispenses bioink layer-by-layer in the printer bed (X-Y plane) by applying a mechanically or pneumatically generated driving force on a cartridge -typically a syringe. During the deposition process, the fluid adopts a cylindrical shape as it starts getting out of the needle connected to the dispensing system. To improve printing accuracy, parameters like extrusion rate, syringe pressure, gauge size, print speed and needle-bed distance have to be considered in different configurations during the setup of the mechanism [19]–[21].

Pneumatic-based systems require compressed air to push the bioink out of the needle. However, this pressurized air dispensed by the air compressor must be filtered and sterilized to minimize the risk of contamination of the bioink [22]. Two configurations are commonly implemented in pneumatic systems: valve-free and valve-based, each one has particular features for different applications [23], [24]. The valve-free configuration has been widely preferred due to its simplicity and compatibility with hydrogels that present shear-thinning characteristics. The valve-based configuration might be considered for high-precision applications due to its on-off switching mechanism regulated by a controller to enable a more accurate pressure and pulse frequency control [25]–[29].

Mechanically-based systems work converting the radial motion of a step motor to linear motion that pushes the bioink through the needle using piston-driven or screw-driven configurations [22]–[24]. The piston-driven configuration uses a lead screw to transmit the movement from the stepper and to a structure connected to the printhead (e.g., a syringe). The screw-driven configuration is preferred when extruding highly viscous materials [30] with the caveat of creating large pressure gradients that may induce forces causing more damage to the loaded cells than a pneumatic mechanism [31].

B. Material Jetting

This process describes technologies in which the material used is selectively deposited in the form of droplets.

1) Laser-Assisted Bioprinting (LB): This non-contact technique is based on the laser-induced forward transfer (LIFT) principle [32], [33]. It uses a laser pulse with an incident beam directed towards a surface, known as the donor slide that transfers a small volume of material to another surface called the receiver slide [34], [35]. The donor slide has three layers: (1) the optically transparent substrate chosen according to the incident wavelength, e.g., glass for near-IR [36], [37] or quartz for ultraviolet (UV) [38]; (2) the absorbing layer or Dynamic-Release-Layer (DRL) [39] to avoid the interaction

between the layer of bioink and the laser pulse, mostly made of a metal such as titanium or gold [36], [40]–[42]; and (3) the bioink layer to get transferred to the receiver slide.

The interaction at the interface between the DRL and the laser pulse generates a vapor bubble at the focus spot. The bubble will expand until it collapses and consequently, induces the formation of a jet of bioink towards the receiver slide. The design of the non-contact technique requires maintaining DNA integrity of the living cells by using appropriate wavelengths, and the ideal rheological properties and the surface tension of the bioink to control bubble dynamics. An adequate collapse that generates the desired jet film thickness requires optimization of parameters like laser fluency (pulse energy/spot area), pulse duration (ranging between nanoseconds, picoseconds to femtoseconds), frequency (Hz) and beam quality [43].

2) Droplet-Based Bioprinting: Inkjet-based bioprinting mechanism is the most accepted modality of the droplet-based bioprinting (DBB) category, which additionally includes: Electro-Hydrodynamic Jetting, Acoustic Droplet-Ejection and Micro-valve Bioprinting. Inkjet deposition of patterned constructs might be accomplished by continuous inkjet (CI) or drop-on-demand (DOD) inkjet. DOD inkjet is preferred because it generates droplets when required, unlike CI due to the Rayleigh-Plateau physical phenomenon [44], [45]. Methods based on machine learning have been developed to study droplet properties such as droplet size and volume to improve deposition precision and stability [46]–[48]. DOD inkjet ejects drops of bioink onto a suitable substrate by overcoming steady and unsteady inertia. In this process, the viscous forces and forces resulting from the surface tension of the bioink are applied by a thermal or piezoelectric stimulus [49]. It is mostly implemented when using low viscous bioinks to avoid nozzle clogging. Thermal-induced droplet formation is produced with a microheating element that heats itself for a short period of time (μ s) when a pulse of current is applied. Later, a layer of liquid in contact with the microheating element is vaporized to nucleate a bubble that expands until it collapses, which generates a build-up pressure that forces the ejection of a droplet [23], [50] similarly to the aforementioned laser-assisted bioprinting technique. Different studies suggest that the use of elevated temperatures for this technique, ranging from 46 °C to 300 °C, maintain high cell viability (89%) and do not significantly affect the functionality of the cells [51]–[53] likely due to the microsecond duration range of the high heat. Piezoelectric-based bioprinting relies on the physical phenomenon of some crystals to undergo mechanical reversible deformations when a voltage is applied. Since the crystal is in contact with the bioink chamber, it deforms synchronously triggering the propagation of acoustic waves, which reach the adequate pressure to expel a droplet [54].

According to ISO/ASTM 52900, there are other processes defined as vat photopolymerization, binder jetting, directed energy deposition, powder bed fusion and sheet lamination. The VAT photopolymerization process, applied under the Digital Light Processing (DLP) modality in the field of bioprinting, is employed in two [55], [56] of the forty-one bioprinted in vitro models analyzed in this article (Tables I–IV). The remaining processes have limited usefulness for current bioprinting applications and therefore, are not addressed in this review. On the other hand, the constant evolution of the field has led to the development of novel processes that do not fully satisfy the current ISO/ASTM classification, as stated by other authors [57], such as sonolithography [58], aspiration-assisted bioprinting [59], the Kenzan method [60] and volumetric bioprinting [61].

III. HYDROGELS AS A BIOINK CONSTITUENT AND BIOMATERIAL INKS

The suitable material for biofabrication, known as bioink, is defined as a formulation of cells suitable for processing by an automated biofabrication technology that may also contain biologically active components and biomaterials. Bioinks must have cells as a mandatory component (e.g., single cells, coated cells or cell aggregates) and an optional mixing component (e.g., decellularized matrix or hydrogels) in contrast to biomaterial inks, which are materials that can also be processed through the aforementioned techniques but do not contain cells while being printed [62].

In this review, a special emphasis is done on hydrogels, which are defined as 3D polymeric networks with extremely high hydrophilicity that allows them to swell or shrink in aqueous environments. They are used in a wide range of biomedical applications [63], [64]. Hydrogel's ability to trap cells and bioactive factors; promote cell adherence, proliferation and growth, providing the necessary conditions to preserve the biological material through the bioprinting process. This type of cross-linking polymers suffers a gelation reaction that holds together their internal structures by covalent bonds, hydrogen bonds, ionic forces, affinity interactions, physical entanglements of individual polymer chains, polymer crystallites, hydrophobic interactions or a combination of any of these [65]. Whether the cross-linking occurs before, during or after printing, affects printing fidelity [66], [67]. Depending on the hydrogel properties, inducing chemical or physical bonding would result in an irreversible or reversible gelation process [68].

A. Natural Hydrogels

Hydrogels can be derived from natural or synthetic sources. Natural hydrogels are derived from biological sources (e.g., marine algae, ECM) and present good biological characteristics such as biocompatibility, biodegradability and low toxicity. The polymers found in nature that have been extensively used as hydrogels are collagen, alginate, hyaluronic acid, gelatin and fibrin.

1) Collagen: It is the major component of the ECM. From the twenty-eighth types identified to date, type I collagen is mainly used for biomedical applications [69] due to its high biocompatibility, low immunogenicity, and its considerable quantity of integrin-binding domains that enable cell attachment, growth and proliferation [70], [71]. It is sensitive to temperature and pH. Neutralizing the pH and the temperature to physiologic conditions is necessary to produce cross-linked hydrogels suitable for extrusion-based bioprinters due to the increase in viscosity that triggers the reaction. Since inkjet-based bioprinters work with low viscous hydrogels, it is preferred to take advantage of the low viscosity of the uncross-linked collagen hydrogel precursor [72]. Collagen hydrogel limitations are related to its behavior at low temperatures (liquid state) and neutral pH or high temperatures (fibrous structure) [73], the slow gelation rate (15-30 minutes) to achieve a solidified state and poor mechanical properties.

2) Alginate: It is a linear polysaccharide derived from cell walls of brown seaweed containing α -D-mannuronic acid (M) and β -D-guluronic acid (G). It has been widely used as a hydrogel due to its natural attributes, high biocompatibility, stability and ability to hold large amounts of water owing to its

high carboxylic acid content [74], [75]. Its cross-linking process is simpler and faster than its counterparts as it only requires the addition of divalent cations (e.g., Ba^{+2} , Ca^{+2} , or Sr^{+2}) to form ionic bonds with the G-blocks providing a gel-like structure. Ionic concentrations and the G/M ratio affect directly the mechanical properties of the hydrogel [76], [77]. Alginate hydrogels are chemically modified by including RGD peptides to improve cell attachment [78]. Limitations are related to degradability due to the absence of the alginase enzyme in mammalian cells preventing degradation of the strands, a process that is conducted by the replacement of divalent cations with monovalent ones leading to a decreased mechanical stiffness [72].

3) Hyaluronic Acid (HA): It is a glycosaminoglycan polysaccharide composed of sequentially bonded disaccharide units of glucuronic acid and N-acetylglucosamine. The highly anionic nature of the linear polysaccharide confers the ability to swell with water creating a volume that provides structural support, promotes cell signaling, wound repairing and matrix organization. Its fast degradation by hyaluronidase and mechanical weakness make chemical modifications necessary for its applicability in biomedical fields. Thiolation (HA-SH) and methacrylation (HA-MA) cross-linking improve their printability [79]–[81]. Frequently, it is used together with collagen, gelatin, methylcellulose, or alginate to produce a bioink with improved mechanical and biological properties [82]–[87].

4) Gelatin: It is a hydrolyzed protein derived from collagen type I characterized by good biocompatibility and poor mechanical stability. The sol-gel temperature-dependent property of the biomaterial determines the applications. Since, it is water-soluble at physiological conditions it may affect viability *in vitro* or *in vivo*. To take advantage of the thermosensitivity of gelatin, it is often used as a sacrificial material for the post bioprinting process. For this purpose, increases above the upper critical solution temperature generate microchannels or porosities in the gaps left after washing [88], [89]. Furthermore, hydrogel precursor of uncross-linked gelatin can be used as an additive for processing to increase the viscosity of the bioink rather than the principal hydrogel component or can be cross-linked through chemical, enzymatic or physical processes to be suitable for a tissue-engineering scaffold [72]. Particularly, the treatment with glutaraldehyde was widely used to modulate the physical-chemical properties of the gelatin [90], but its use is limited because of calcification and cytotoxicity [91]. New cross-linking methods such as photoreticulation after a methacrylation reaction stands out because it correlates the elastic and the viscous modulus with the degrees of GelMA during its fabrication [92]–[94].

5) Fibrin: This fibrous protein derives from the protease thrombin cleavage on fibrinogen, in presence of Factor XIII [95] or genipin [96], [97]. The fibrin matrix is cross-linked enhancing a stable polymer that is involved in natural wound repairing processes, has good cell adhesion capabilities and cell recruitment, promotes angiogenesis and is typically used in surgeries as a sealant [98]. A fibrin-based hydrogel could be suitable for tissue engineering applications due to the aforementioned biocompatibility. However, it lacks of good mechanical properties and long-term stability as degradation (fibrinolysis) happens within hours (*in vivo*) or in a week (*in vitro*) by the action of the plasmin enzyme [72]. Efforts to slow degradation rates and enhance mechanical properties include the manipulation of pH, calcium ions, fibrinogen or cell density concentrations, as well as the addition of plasmin inhibitors [95], [99], [100].

B. Synthetic Hydrogels

Synthetic hydrogels are increasingly used thanks to advances in tunable mechanical properties, processing ability and the capability to modify their chemical structure to reach a favorable biocompatible environment for cells such as natural hydrogels.

1) **Poly(Ethylene-Glycol):** It is a hydrophilic, water-soluble, biocompatible and biological inert polymer of ethylene oxide [101]. PEG backbones can be structurally linear or branched (star or multi 3-, 4-, 6-, 8- armed) [102], [103] and easily cross-linked by a thermally or photoinitiated induced polymerization with macromers such as diacrylate (DA), methacrylate (MA), vinyl sulfone (VS) to form a PEG-based hydrogel [104]. It is also known as PEG when the polymer consists of molecular weights less than 20 kDa, poly (ethylene oxide) PEO for greater than 20 kDa or poly (oxyethylene) in general due to the effect that has its molecular weight over the mechanical and degradation properties of hydrogels [72], [105], [106]. The major feature of PEG is its capability to be easily tailor-made to include functional groups, bioactive molecules [107]–[110], adhesive RGD peptide sequences to facilitate the adhesion and short peptide sequences derived from ECM proteins to improve its biological and mechanical properties [111], [112].

2) **Poloxamers:** They are composed of non-ionic copolymers with a hybrid structure in terms of their affinity for water, where a hydrophobic polyoxypropylene (PPO) block is located between two hydrophilic polyoxyethylene (PEO) blocks, thus forming an A-B-A triblock structure. Also known as the trademarks Pluronic, Synperonics or Kolliphor, these synthetic polymers have been widely used in the biotechnology industry due to their amphipathic nature which gives them the surfactant capacity to form micelles [113], [114]. For biological manufacturing purposes, Pluronic (particularly Pluronic F-127) has been used as a sacrificial hydrogel and when printing biocompatible constructs [115]–[117]. Enzymatic, chemical and radiation methods have been implemented for cross-linking. The most accepted reversible mechanism is the temperature-dependent one that produces gels between 10 to 40 °C [118], [119]. Also, decreasing temperature below the lower critical solution temperature promotes transition to a liquid state whose solubility in water and organic solvents makes it useful in the manufacture of structures with complex architecture [120], [121]. Biological limitations include low cell adhesion and cytocompatibility, which directly affect cell viability. Therefore, modifications such as the addition of polysaccharides [122], oligo(peptides) [123] or RGD motifs [124] have been implemented to promote biocompatibility. In addition, its preparation in different media such as phosphate-buffered saline or Dulbecco's Modified Eagle Medium can reduce the critical freezing temperatures for different polymer concentrations. For instance, 25% w/v is the best candidate for a bioink due to its rapid gelation at 37 °C, adequate viscoelastic properties, pseudoplastic behavior and rapid recovery of viscosity after shearing [125].

IV. MECHANICAL PROPERTIES OF BIOINKS AND BIOMATERIAL INKS

Broadly speaking, a thorough understanding of the mechanical properties of materials allows us to characterize and compare them for different applications. Specifically, either for bioinks or biomaterial inks, there are a number of properties that play an essential role when adjusting and controlling the printing parameters.

A. Viscosity

The viscosity of a hydrogel is a primordial property for the manufacturing process since it determines the resistance of the material to flow, being directly related to the applied pressures in each bioprinting method. To handle the viscosity of the bioink (or biomaterial ink), parameters such as temperature (inversely proportional); molecular weight, cell density or polymer concentration (directly proportional) can be modified [126]–[128]. However, a delicate balance needs to be achieved to maximize cell viability [129] while achieving an adequate viscosity. Low viscosity hydrogels do not affect the cell environment when shear stress is applied because they require less pressure to be dispensed, but their constructions tend to be watery and softer without the ability to maintain their shape after printing [126]. On the other hand, high viscosity hydrogels confer stability to the bioprinted structure but may represent a risk to cell viability when the pressure applied to dispense the material is higher [130]. In that sense, the literature reports certain specific viscosity ranges for each technique. The EBB technique, it is compatible with highly viscous formulations ranging from 30 to 6×10^7 mPa·s. For example, it is the main technique used to deposit polycaprolactone (PCL), a synthetic polymer normally used as the structural component of the *in vitro* bioprinted platforms (e.g., chips, transwell systems) due to its high viscosity [131]–[133]. In the case of the DOD or LAB techniques, the selected formulations should exhibit low (<12 mPa·s) or moderate (1–300 mPa·s) viscosities, respectively [134], [135].

Therefore, it is necessary to consider the effect of cell density on the viscosity of the bioink and also to perform rheological evaluations in order to define an appropriate viscosity so better printability results can be achieved [136], [137].

B. Shear Thinning

The behavior of fluids under shear stress may vary depending on whether they are Newtonian or Non-Newtonian fluids. The shear-thinning behavior of non-Newtonian hydrogels can determine a high printing fidelity [138]. In these materials, increased shear rate induces the uniform reorganization of the polymeric chain conformation, parallel to the direction of the applied stress causing a non-linear decrease in their viscosity [139], [140]. The molecular interactions responsible for this behavior are the physical associations and dynamic covalent chemistry [141]. Therefore, shear-thinning is widely used in extrusion-based bioprinters to allow the deposition of high viscous hydrogels, which gives them stability and good mechanical strength when they come out of the nozzle since they recover their viscosity due to the absence of shear stress. However, properties such as fracture resistance, biocompatibility, tunable release and cytoprotective behavior must be improved while maintaining thinning, as well as self-healing behavior to increase their use for *in vivo* models [141].

It should be considered that the term is commonly confused with thixotropic behavior because of the similarities of the *stress versus strain* and *viscosity versus shear rate* graphs [142]. Discriminating between those phenomena proves difficult due to the combined shear and time effects in their measurement [143]. However, the shear-thinning phenomenon is associated with a rapid recovery close to zero time [144] of the fluid viscosity in the absence of shear stress while the viscosity of a thixotropic material should be a function of the duration of the applied shear stress.

C. Swelling

This property is strongly dependent on environmental conditions of pH and temperature. In pH-sensitive hydrogels [145], changes of pH based on the pKa and pKb of the ionizable groups alter the hydrophilicity of the polymer chains by inducing an increase in the electrostatic repulsions between the chains and consequently the swelling of the hydrogel [146]. Temperature is an important factor that influences the mechanism of hydrogel formation and the properties of the hydrogels during optical polymerization, enzymatic reactions, physical, ionic crosslinking, among others [147]. As mentioned previously, temperature-sensitive hydrogels such as gelatin and poloxamers respond to thermal stimuli either by increasing or decreasing the temperature above or below their critical solution temperatures [148].

Water absorption of hydrogels influences the diffusion of different essential factors such as nutrients, oxygen, growth factors through the unbound regions of the macropores and gaps. Chaotropic agents affect water absorption by direct interference with hydrogen bonds destabilizing the polymer structure and making it more sensitive to any applied stress [149], [150]. Also, the degree of swelling of the hydrogels is mainly determined by the cross-linking ratio through an inverse relationship because it hinders the mobility of the polymer chains.

The swelling behavior of hydrogels for bioprinting applications may affect unfavorably the deformation and diffusion capabilities or may change the geometry if more than one type of hydrogel is implemented within the same construct. Swelling is typically quantified by measuring the rate of change between weight after (hydrated) and before (dehydrated) immersion in water or some standardized solution [151].

D. Yield Stress

Yield stress is the maximum limit to apply stress without initiating the flow of the material. It means that any pressure above the yield stress value will trigger the polymer solution to flow. It is associated with shear stress since it is necessary to reach a certain pressure to start the deposition of the material. With higher yield stress values, the shear stresses become higher and harmful to the cells. Three methods have been explored to determine the yield stress value: (1) extrapolation of the flow curves at low shear rates, (2) the Bingham equation, and (3) the Modified Bingham equation. Being the third one, the most commonly applied as it fits better to the experimental data of the hydrogel formulations [152], [153].

V. TISSUE MODELS FOR SAFETY TESTING

In this section, we discuss studies that developed structures to model human physiological and pathological states of cardiovascular tissue, liver, cancer and skin using bioprinting strategies. The advancement in these types of engineered living systems is considered a natural progression of the different stages of bioprinting development towards establishing it as a critical technology in tissue modeling [154].

A. Liver Models

The liver is an organ whose main function is to maintain metabolic homeostasis through processes such as glycolysis, gluconeogenesis, ureagenesis, glycogen synthesis, triglyceride

synthesis, β -oxidation and lipogenesis. Also, it is made up of different types of cells including hepatocytes, stellate cells, sinusoidal endothelial cells, Kupffer cells, and cholangiocytes. The bioprinted models described in Table I contemplate a variety of microstructures designed to maintain both the cellular distribution and the microarchitecture of functional units responsible of physiological or pathophysiological conditions. EBB was the most commonly used technique to fabricate these models.

A large heterogeneity of cell lineages is used as bioinks to bioprint. Much effort to characterize and develop hybrid bioinks ideal for liver-mimetic microenvironments focus on improving rheological properties, while hybridization with nanoparticles or polymers aims to yield bioinks with high printing fidelity [87], [155].

Being the liver the main organ responsible for drug metabolism, there are microscale platforms employing liver tissue-derived cells that serve as high-fidelity drug metabolism models. Chang et al directly bioprinted tissue constructs composed of HepG2 cells and alginate on a PDMS microchip to develop a 3D microfluidic tissue chamber unit [156]. A highly precise non-commercial bioprinter extruded tissue constructs in a liver-like sinusoidal micro-pattern. The hepatocytes of the micro-organ device metabolized a fluorogenic substrate that was perfused to assess their metabolic function and showed an increase in the percentage of metabolic conversion of the drug when compared to non-perfused controls. Static culture conditions also were employed to determine parameters such as the alginate concentration and media volume, which showed no effect on the percentage of drug being metabolized.

Bioprinting techniques that maintain pluripotency or do not trigger, change or interrupt a stem cell differentiation process, have the potential to revolutionize personalized medicine by producing tissues on-demand or human-derived constructs for drug development. Liver bioprinted constructs using hESC-derived HLCs have been shown to preserve moderate viability post-bioprinting process [157]. The technique used for cell deposition was DOD and by using short-length nozzles, the exposure time of the cells to shear stress was reduced favoring its viability, as shown in previously reported simulations using mathematical predictive models and experimental results [158].

Complex platforms have been developed integrating human hepatocytes or hiPSC-hepatic progenitor cells with non-parenchymal (or supporting) cells such as hepatic stellate cells, endothelial cells and adipose-derived stem cells [55], [159]–[161]. Some of these platforms recapitulate the inherent multicellular architecture of liver tissue at the micrometer level while others provide evidence that liver-specific functionality at cellular, molecular and histological levels was improved in comparison with traditional 2D cultures. For example, a complex bioprinted 3D in vitro model served as a platform to investigate the expression levels of some key enzymes in the metabolism of drugs from the cytochrome P450 (CYPs) family after treatment with rifampicin [55], which is a drug commonly used in the treatment of tuberculosis with a potential risk of causing hepatotoxicity [162]. The findings showed a significant increase in CYP expressions compared to non-drug treated controls when the multicellular platform (complex) was used, however, no significant differences were observed when two-dimensional cultures or three-dimensional single-cell (simple) models were used. Similarly, another 3D bioprinted complex platform [159] has been used to evaluate its ability to model drug-induced liver injury in comparison to a standard hepatocyte monolayer culture

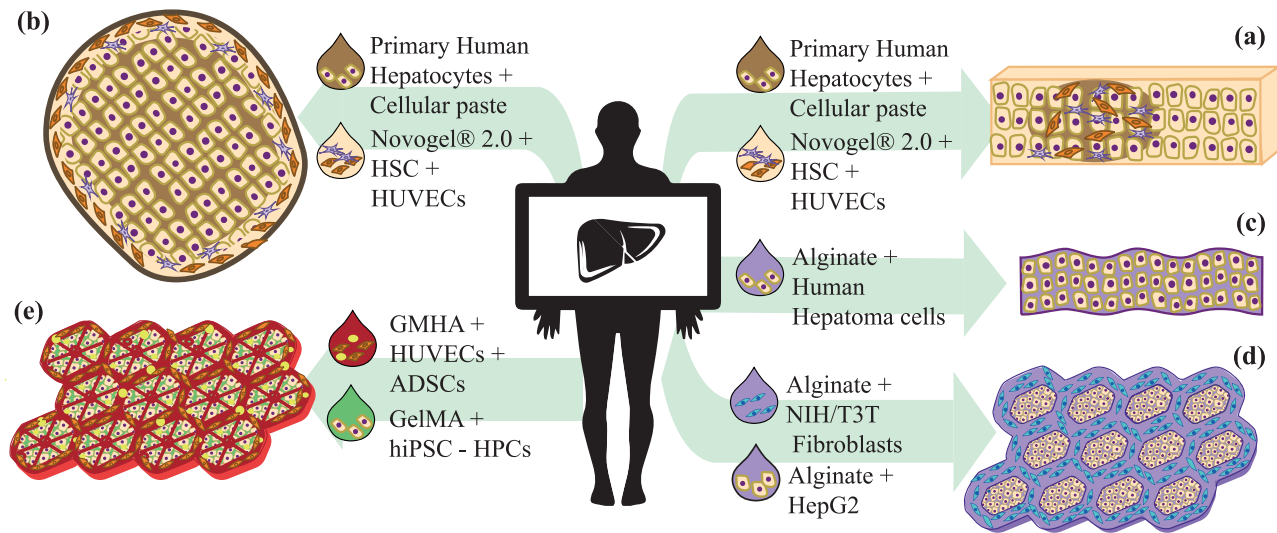


Fig. 1. Schematic illustrations of five liver bioprinted models included in Table S1 detailing their cellular distribution and bioinks: (a) [161], (b) [159], (c) [156], (d) [155], and (e) [55].

after exposure to Trovafloxacin, a drug withdrawn from the market due to its induction of hepatotoxicity [163]. In response to clinically relevant dose treatment, the two-dimensional culture maintained its ATP and albumin levels while the 3D model demonstrated a high sensitivity showing significant decreases in both markers, which supports its ability to predict clinical hepatotoxicity.

Fig. 1 summarizes the structural configuration of these models and a more detailed analysis of them is provided in Table I.

B. Cancer Models

Cancer develops in almost any tissue and comprises more than 100 types of diseases with unique microenvironments. Bioprinted cancer models present a number of advantages including: 1) spatial control of matrix properties that include stiffness and diffusion of biochemical factors, 2) integration of perfusable vascular networks, and 3) automated high-throughput fabrication [164], [165]. Current models recapitulate cell-cell and cell-ECM interactions, chemical (growth factors, cytokines, nutrients, oxygen, pH, drugs) and physical gradients (ECM stiffness and strain, electric field, interstitial flow shear), and recruitment of other cells; all of these features are known contributors to the complexity of 3D tumor microenvironments [166]. To date, bioprinted malignant solid tumors (i.e., masses that do not contain cysts or liquid areas) include those of the nervous system [167]–[170], liver [171], [172], lung [173], [174], breast [175], [176], pancreas [176], [177], ovaries [178], and cervix [179], [180] as summarized in Table II.

The promises of personalized medicine using bioprinted tumors might be the next great breakthrough when deciding treatment strategies [181]. However, few *in vitro* models have been developed with patient-derived cells [170], [171], [176]. Yi *et al.* presented a patient-specific on-chip platform using patient-derived glioblastoma cells and endothelial cells, each immersed in Brain-DECM as a bioink. The concentric structure was designed to promote interaction between cancer cells and the stromal region, as well as to generate oxygen gradients.

The authors demonstrated that the model accurately reproduces patient-specific treatment responses with concurrent chemoradiation and temozolomide treatment [170]. Xie and co-workers employed patient-derived hepatocarcinoma cells (HCC), gelatin and sodium alginate to bioprint 3D HCC models. The constructs retained the tumorigenic potential, histological properties, genetic alterations and expression profile of the corresponding original patient tumor during a long-term culture [171]. Langer *et al.* bioprinted multicellular scaffold-free structures using patient-derived cancer cells and stromal cells such as fibroblasts, adipocytes or HUVECs to develop breast and pancreatic cancer tumor models that allowed the study of tumorigenic phenotypes, cell migration and proliferation, and ECM deposition in response to extrinsic signals or therapy [176]. Fig. 2 illustrates some of the models detailed in Table II using EBB to maintain high cell viability in the post-printing stage (i.e., day 0).

C. Cardiovascular Models

Cardiovascular toxicity is a leading cause of drug attrition in pre-clinical and clinical stages [182]–[184]. Therefore, there is a high pressure to identify toxic compounds as early as possible during development to reduce the associated economic impact. When it comes to drug discovery, *in vitro* high-throughput screening (HTS) is a well-established method that primarily evaluates the metabolism, pharmacokinetics and toxicology of hundreds or thousands of drug compounds at high speed in 96-well or grater arrays. Bioprinting is a tool that can complement HTS by providing reproducibility, complexity, and micrometer accuracy during deposition [185].

DLP-based bioprinting was used to create bioprinted cardiac micro-tissues as an auspicious candidate for HTS [56]. This platform contained cardiomyocytes (CMs) derived from human induced pluripotent stem cells (hiPSCs) which exhibited an increased expression of markers of mRNA maturity when compared to two-dimensional cultures. Also, it demonstrated a higher degree of alignment, and a faster time to start beating as a fully differentiated tissue by the seventh day of post-bioprinting

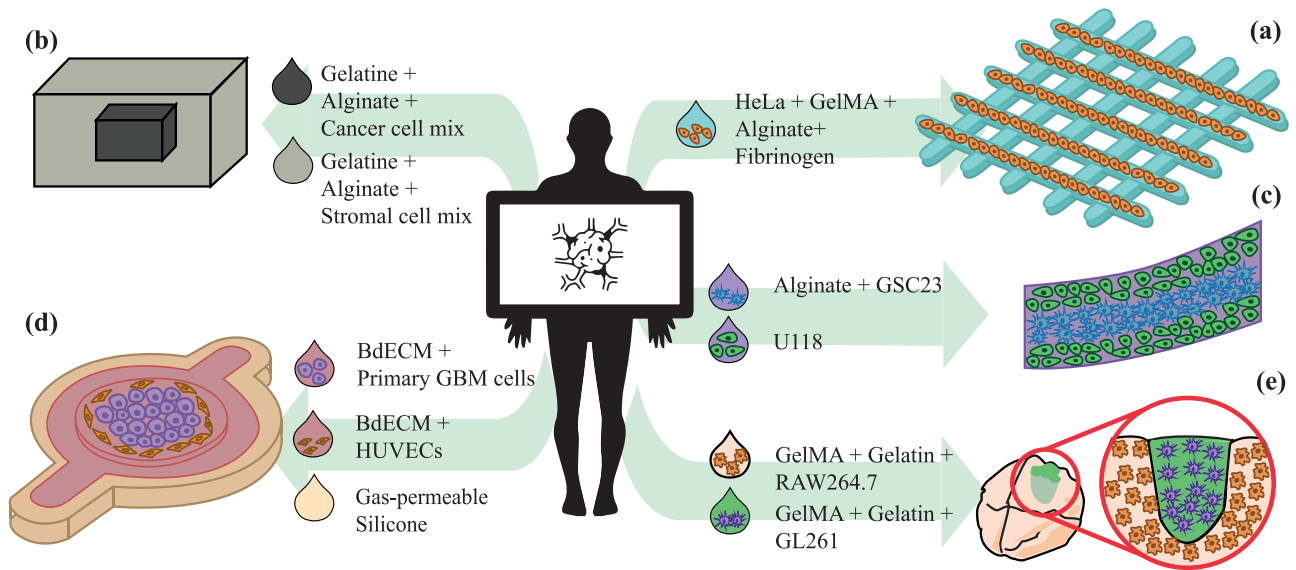


Fig. 2. Schematic illustrations of five cancer bioprinted models included in Table S2 detailing their cellular distribution and bioinks: (a) [180], (b) [176], (c) [169], (d) [170], and (e) [168].

culture. Human Ventricular Cardiac Fibroblasts (HCFs) were also included in the bioprinted construct and formed a compact tissue with the hiPSC-CMs along seven days of post-bioprinting culture. This bioprinted model is expected to be used in a variety of applications including patient-specific disease testing because it is constituted by hiPSC-CM and multi-organ-on-a-chip platforms since it can be printed on a coverslip.

Myocardial tissue engineering also involves developing disease models to replicate the pathophysiology at a structural, mechanical and electrical level of the native tissue. For example, a spheroid-based hetero-cellular platform has been developed to mimic contractile output and electrical synchronization. Alterations of these structural features are distinctive of scarred cardiac tissue that arises after myocardial infarction [186]. The platform composed of iPSC-CMs spheroids and HCFs spheroids was precisely bioprinted using a novel non-conventional aspiration-assisted method [59] and a self-healing hydrogel. Unlike previous *in vitro* models, this platform lacked the anisotropic alignment characteristic of mature myocardium. Unfortunately, both platforms lacked vascular networks hindering their long-term survival due to the absence of nutrients and oxygen.

In this context, Zhang and co-workers engineered an endothelialized myocardium platform composed of HUVECs and hiPSC-CMs that replicates the maturation, alignment and contraction of native tissue. When exposed to doxorubicin, a common anti-cancer drug, cardiomyocytes beating rate was reduced from 94.5% to 2.78%, and the expression of von Willebrand factor (vWF) on endothelial cells was reduced from about 100% to close to 40%, following an expected dose-dependent response [187]. It should be noted that the manual seeding process of the hiPSC-CMs on the HUVECs-laden scaffold could be optimized by bioprinting these cells in order to have greater spatial control and homogeneous distribution. Also, the use of sacrificial biomaterial inks would facilitate the perfusion of the construct, which was not achieved because the HUVECs-laden microfibers were not hollow.

Vascular models have also gained relevance because of their role in common pathologies such as cancer and its metastatic

process, and tissue ischemia. Depending on the application, different types of structures are required to be developed for each type of vascular channel (i.e., capillaries, arterioles/venules or larger vessels). The coaxial extrusion bioprinting technique combined with sacrificial biomaterial inks (e.g., Pluronic F-127, Gelatin) is a widely used tool to develop hollow tubular constructs [188], [189]. By using this, researchers have developed a vascular model that mimics the physiological functions of native endothelium such as selective permeability, antiplatelet adhesive effect, preservation of vWF in the cytoplasm of HUVECs, shear stress gene expression regulation and capillary sprouting in presence of directional proangiogenic stimulations [190]. The use of this platform was expanded to be a disease model by incorporating airway epithelial inflammatory cytokines in the culture medium and demonstrated high expression of cell adhesion molecules typical of inflammatory processes (ICAM-1, E-Selectin) as well as the breakdown of endothelial junctions. A DOD bioprinted construct demonstrated cell viability larger than 83% and resembled the mechanical behavior and biological properties of native vessels [190], [191]. This construct included additional vascular cells that promote the stabilization and maturation of vascular conduits such as smooth muscle cells and fibroblasts. Fig. 3 shows the structural components of some of the different constructs built to develop cardiovascular similes for cardiotoxicity screening (Table III).

D. Skin Models

While being the largest organ of the body, the skin represents the first defense barrier against external pathogens serving as an important delivery route for pharmaceutical and cosmetic applications.

Structurally, the skin conformation includes three main layers (i.e., epidermis, dermis and hypodermis) that are characterized by different biological and mechanical functions. Conveniently, current bioprinting methods work on the principle of layer-by-layer deposition of bioinks and furthermore, skin is considered a tissue of lower complexity when compared to other constructs

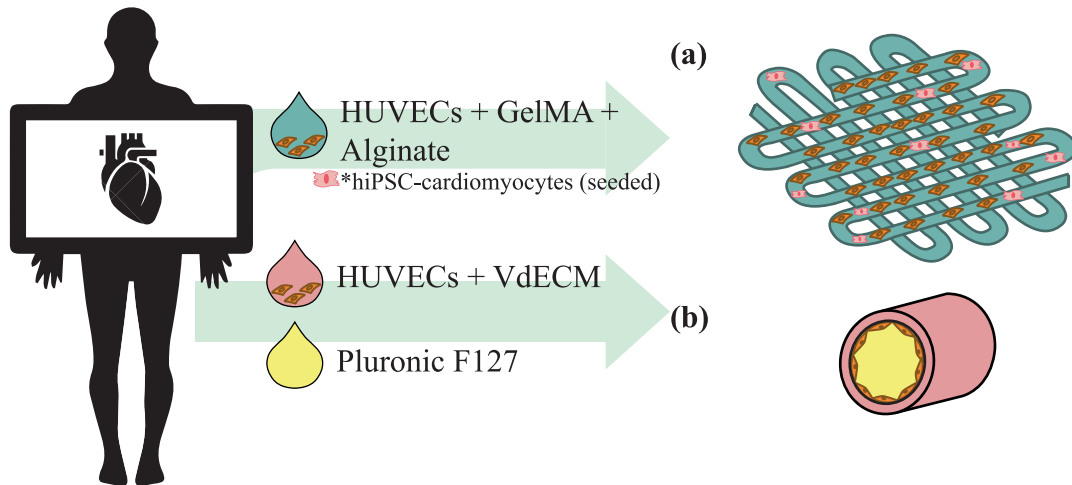


Fig. 3. Schematic illustrations of two cardiovascular bioprinted models included in Table S3 detailing their cellular distribution and bioinks: (a) [187] and (b) [190].

such as hollow tubes (blood vessels), non-tubular hollow organs (bladder) or solid organs (kidney) [135].

Several key cell types such as keratinocytes, fibroblasts, adipocytes, melanocytes, immune system cells, nervous system cells and capillary cells populate permanently or temporarily different regions of the skin microarchitecture [192]. Despite this, the *in vitro* models reported in the literature and reviewed in this article predominantly employ keratinocytes and fibroblasts in their bioinks due to their abundance in either the epidermis or dermis [132], [193]–[202]. Although all models recapitulated the physiological properties of the skin, each research group employed a unique strategy to develop the different platforms. For instance, through a hybrid bioprinting system (i.e., extrusion and inkjet techniques), Kim and coworkers engineered a 3D human skin model using a single-step process [132] and also demonstrated the potential of skin-dECM as a high-fidelity bioink that provides a favorable microenvironment for the epidermis and dermis [194]. Techniques such as LAB have also been implemented to construct skin-equivalent multicellular models either to study the tissue formation process [196] or to analyze its response to cosmetic treatment [199].

The dermal-epidermal junction (DEJ) has been extensively studied however few bioprinted *in vitro* models have aimed to replicate the complex anatomy of this junction. It is crucial to reproduce this type of structure because it plays an important role in physiological and pathophysiological processes of the skin: its undulating morphology acts as a barrier for molecular transfer and cell migration between layers, it provides mechanical support to the epidermis and, DEJ fixates the epidermis and dermis [203], [204]. Admane and coworkers used EBB to engineer a DEJ simile by strategically fitting epidermal layers on the dermal layers in structurally complementary patterns [195].

The incorporation of multiple skin appendages in *in vitro* skin models is relatively uncommon despite their known protective function and involvement in homeostasis processes, thermoregulation, among others [205]. In that sense, Zhang and collaborators developed a platform that included sebaceous glands and hair follicles using the EBB technique and spheroid culture [200]. This *in vitro* model allowed the analysis and understanding of the complex crosstalk between the two appendages.

Furthermore, it represents a starting point towards a fully functional model whose potential application can be extended to model common skin appendage disorders [206] or to study drug delivery processes via hair follicles [207], [208]. Similarly, there are few developments of 3D skin models that include melanocytes in their conformation despite their fundamental role in skin pigmentation either uniformly [201] or non-uniformly (resembling skin freckles) [202]. These bioprinted *in vitro* skin models still represent an unexplored field for drug testing or personalized medicine applications.

The skin vascular network is primarily distributed at different levels of the hypodermis and the dermis. In addition to providing nutrients and oxygen and participating in the elimination of metabolic wastes as in most tissue, the cutaneous vasculature plays a vital role in the acute and chronic inflammatory processes of the skin associated with different diseases such as psoriasis, rosacea, atopic dermatitis (AD), alopecia areata, among others [209], [210]. Among these diseases, AD has been successfully recapitulated in a bioprinted model of vascularized skin. In addition to fibroblasts and keratinocytes, typical cells of the dermal vasculature such as iPSC-ECs and pericytes were included. Notably, the increased expression of a common cytokine in late and chronic stage patients (INF- γ) was found only in the vascularized models, which suggested that the inclusion of these cells is necessary to develop a more complete model of AD disease. The model also demonstrated other typical features of the disease such as spongiosis and hyperplasia and the expression of differentiation proteins. Additionally, it was pharmacologically validated with clinical therapeutic data [211].

The aforementioned models do not have a subcutaneous layer included in their structure. This layer composed mainly of adipocytes serves as a thermal insulator, an energy source, provides mechanical support and plays a role in metabolic and endocrine processes through the production of biomarkers such as adiponectin and leptin [212], [213]. Despite this, few studies have included a hypodermal compartment as part of their physiological and pathophysiological triple-layered bioprinted skin models. A physiological model demonstrated that the presence of mature adipocytes could be associated with an increased expression of K19 in the epidermal compartment compared to

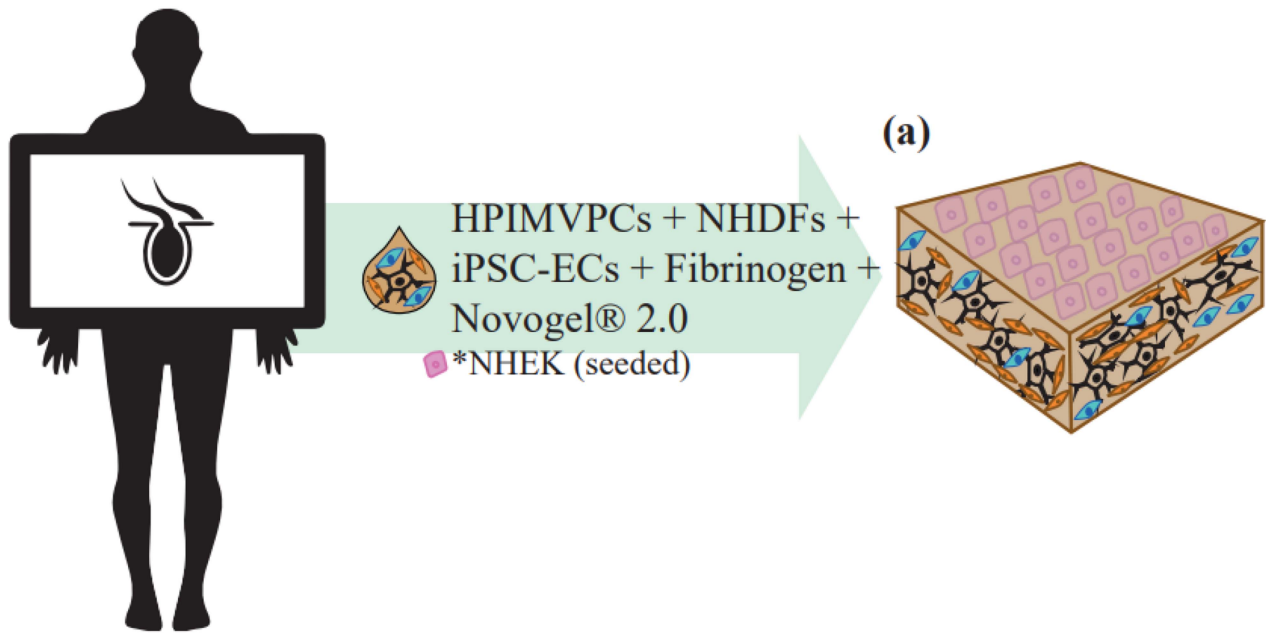


Fig. 4. Schematic illustration of a skin bioprinted model included in Table S4 detailing its distribution and bioink [211].

a dermal-epidermal model [214]. On the other hand, a pathophysiological model which contained a diabetic hypodermal compartment confirmed typical hallmarks of diabetes such as insulin resistance and adipocyte hypertrophy [215]. This model also proved that the interaction between diabetic fibroblasts and normal keratinocytes induced the differentiation of the latter as an epidermis with diabetic properties. Both advanced models were vascularized and perfusable, however, they included a straight vascular channel which did not allow sufficient oxygen and nutrients to be supplied to the more distant cells.

Broadly speaking, bioprinted skin models take advantage of different techniques (Table IV) including EBB, DBB, and LB, with DOD being preferred when depositing keratinocytes that were mostly embedded in their own medium without the need for some biomaterial matrix (Fig. 4).

Each of the bioprinted constructs described in this section must undergo a maturation process before being used as a functional *in vitro* model. For this purpose, static or dynamic culture conditions are used, parameters such as incubation temperature, humidity and CO₂ percentage, culture time are controlled and a specific medium is provided according to the type of cell (or cells) being worked with. In fact, some researchers cross-link the polymeric component of the bioink after the bioprinting process and prior to initiating the maturation culture. Both liver and cancer models addressed in Sections V-A and V-B were cultured under static conditions, in contrast to almost all cardiovascular and skin models covered in Sections V-C and V-D that were post-processed under dynamic perfusion conditions. Custom-made bioreactors and peristaltic pumps were used in the postprocessing of some cardiac constructs to either provide the native perfusion microenvironment of the vascular conduits [190], [191] or to supply nutrients and oxygen to the cardiac tissues increasing their long-term viability [187], [190], [191]. Some of the skin models used embedded bioprinted transwell systems [132], [214], [215] or commercial transwell inserts [193], [195], [198], [202], [211] in their post-processing to place them under an air-liquid interface for epidermal stratification.

Altogether, the constructs described here as technological products show great promise; they are far from being available for clinical use and commercialization. Fig. 5 summarizes the current state of development of the tissue-engineered products.

Despite the exponential growth of academic publications in the development pipeline, the technology readiness level needs to be further advanced to generate greater investor confidence and attract more funding [216]. The technology transfer efforts of short-term applications such as bioprinting *in vitro* models are essential for the rapid adoption of the technology. The acquired experience would serve well when translating to the clinic and facing ethical, social, regulatory or political challenges of long-term applications [217].

VI. FUTURE DIRECTIONS

Current limitations of the constructs are mainly due to structural or functional aspects. Future work should consider addressing how to optimize heterogeneity in an effort to cover the need for functionality obtained from cellular diversity while maintaining a tight control of differentiation and reproducibility. Also, the cell-specific requirements of dynamic interactions with their microenvironment limit the tissues that can actually be successfully designed and implemented. Accomplishing the desired complexity of the microstructure that arrives from the increased dimensionality needs to be carefully designed to avoid obscuring the tissue characteristics that are being studied. Finally, we have a limited understanding about finding the metabolic balance necessary to construct multiorgan platforms. In the following lines, we detail current efforts addressing these limitations that are yet to be implemented into successful models of exposure and disease.

A. Heterogeneity

Cellular diversity is crucial when designing *in vitro* models of exposure or disease that are representative and informative of the

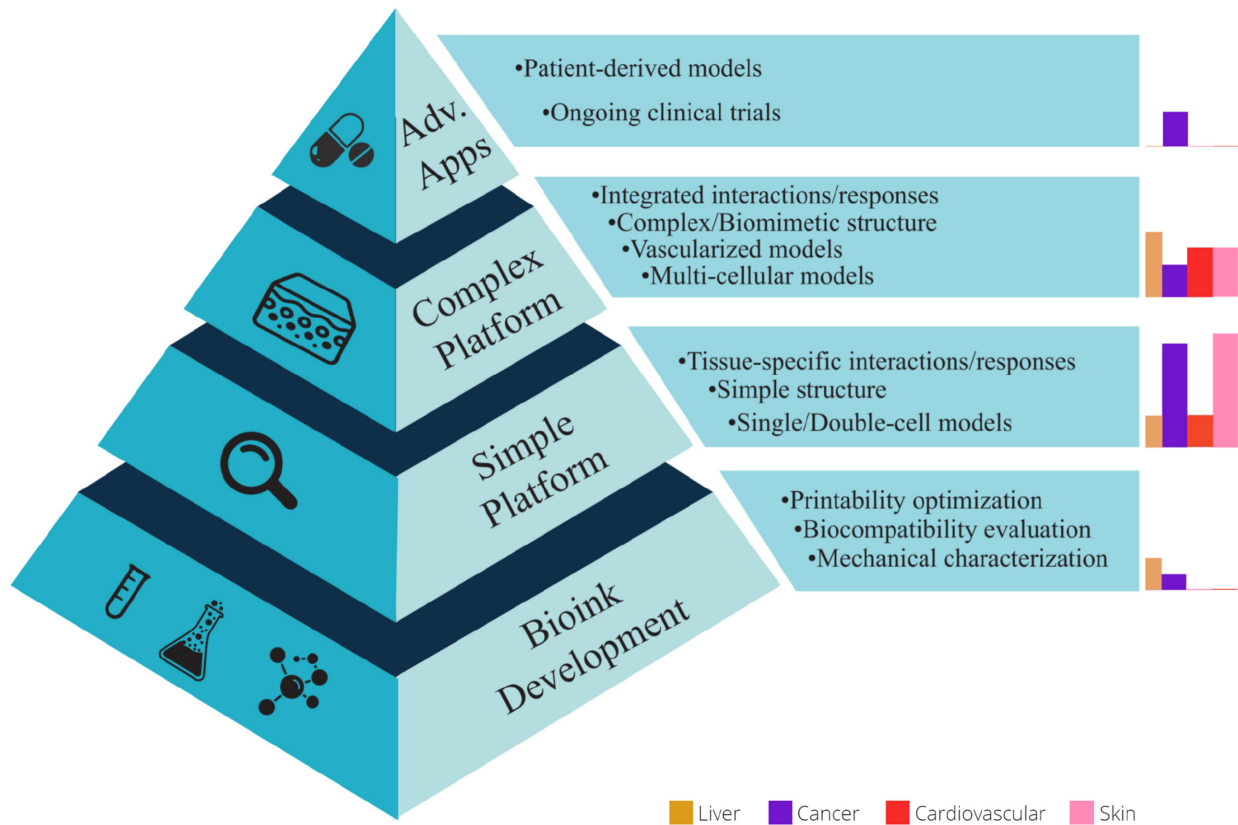


Fig. 5. Classification of the reviewed publications according to the stage of development. The lower level includes studies that formulated, characterized novel bioinks and defined printability requirements to optimize the bioprinting process [87], [155], [174]. The following level includes bioprinted platforms with one or two cell types, with simple structure and/or used to study tissue-specific interactions or responses [132], [156], [157], [168], [169], [173], [175], [177]–[180], [187], [190], [193]–[202]. The next level includes *in vitro* models developed with two or three cell types (in some cases vascularized) with higher structural complexity and/or used to study integrated interactions or responses [55], [56], [159]–[161], [167], [172], [186], [191], [211], [214], [215]. The upper level is the most advanced level which includes complex models developed with patient-specific cells that can be used to measure their correlation with the outcomes of pharmacological treatments applied to the same patient [170], [171], [176]. Thus determining an approach to personalized medicine. The bars on the right indicate the number of models at each stage: brown (liver models), purple (cancer models), red (cardiovascular models), pink (skin models).

specific structure to be modeled [218]. Therefore, it is important to analyze prior to bioprinting the identity and location of the cells that make up the tissue or organ of interest [219]. Integration of immune, vascular and nervous cells into bioprinted models is expected to accomplish more relevant physiological or pathophysiological behavior of the constructs. Default bioprinting setups are not able to deposit multiple bioinks. Therefore, they need to be modified with additional features or procedures such as adapting multiple print-heads in the case of DBB/EBB or excessive manual handling either by the repeated pipetting of the bioink in the case of stereolithography (SLA) or the continuous coating of the donor slide in LB technique. Optimizing these modifications may decrease costs, hardware size and time of fabrication.

The adaptability and versatility of EBB enable the incorporation of a great number of combinations of bioinks/biomaterial inks/cross-linking strategies for extrusion. Coaxial bioprinting being either bi-, tri- or tetra-layered [189], [220], [221] allows the concentric and simultaneous extrusion of multiple materials. Indeed, the fabrication of hollow tubes that function as vasculature [190], [222], [223] has taken advantage of sacrificial biomaterial inks such as alginate or Pluronic F-127. Also, coaxial bioprinting is used when studying self-assembly and interactions between

parenchymal and stromal in shell/core fiber structures [169], [224].

Methods based on chaotic flows can create an interspersed, reproducible and deterministic lamellae cross-section, in which the number of interfaces increases exponentially according to the number of helicoidal elements of the Kenics Static Mixer (KSM) [225]. Notably, the internal organization of the lamellar microstructure is determined by the number of inlets and KSM elements implemented in the KSM. In terms of multi-material bioprinting, a single four-element KSM printhead reached up to manufacture fibers made of four different types of materials [226]. *In silico* CFD simulations have predicted the potential of chaotic flows to create skeletal muscle tissue models made of fibers and highly vascularized.

B. Dynamism

Post-printing physiological health is a critical requirement when developing advanced *in vitro* models and bioreactors. However, recreating the mechanobiology of physiological conditions under static conditions affects *in vitro* models of organs such as the stomach, intestine, or conducts such as the esophagus or the ureters which are characterized by their

peristaltic movement [227], or the heart, bladder and the lungs that are in permanent contraction and relaxation. A new modality of additive manufacturing technology known as 4D bioprinting is emerging as the one that could potentially recreate those complex dynamic microenvironments [228], [229]. The fourth dimension included is the temporal one, and its mechanism approaches the responsive behavior of specialized ‘smart’ materials triggered by external stimuli such as water or even humidity [230], temperature [231], pH [232], magnetic fields [233] or light [234], [235]. It is printer-independent since either extrusion-, inkjet-, or laser-based bioprinters can be used to develop 4D bioprinted constructs. The behavior of the construct can be prescribed and depending on the smart material used it can undergo changes in size, shape, or functionality simultaneously without being harmful to the cells embedded within them.

C. Complex Microstructures

The structural stability of the bioprinted constructs is mainly determined by the mechanical properties of the bioink which enables the patterning of simple geometries (e.g., gridded, circular, unidirectional tubular) to recreate an *in vivo* microenvironment. However, as the complexity of the structure increases in terms of its dimensionality (from 2D to 3D), there is a higher weight to be supported by the base of the construct. The base may consequently collapse or deform, in particular when working with materials of an elastic modulus lower than 100 kPa [236].

Several groups have developed advanced bioprinting methods to address this drawback. For instance, using “freeform reversible embedding of suspended hydrogels” (FRESH). In FRESH bioprinting, bioinks can be extruded inside a support bath due to its Bingham plastic behavior, for which the non-Newtonian fluid does not flow until a yield stress threshold value is reached. The support bath material is made of gelatin microparticles that are surrounded by an interchangeable fluid phase with cross-linkers such as pH neutral buffers, Ca^{+2} or some of their combinations. Constructs with inner and outer complex geometries include the internal trabeculations of a five-day chick heart, a human brain with its sulci and gyri on its surface, coronary vascular networks, heart valves and ventricles [237]–[240].

Beyond adding features to existing techniques such as FRESH with EBB, a light-based bioprinting technique characterized by a simultaneous entire plane photo-polymerization (layer-by-layer) enables highly fast bioprinting of complex micro-architectures [241] such as multi-vascular networks and functional intravascular topologies [242], and liver structural units [55]. Digital light processing (DLP)-based bioprinting working principle relies on the directional projection of light onto a photo-sensitive bioink by a digital micro-mirror device (DMD) which consists of millions of micro-opto-electro-mechanical addressable micro-mirrors that selectively rotate according to the layer-by-layer input patterns or digital masks [243]. Furthermore, as it is a nozzle-free technique, it avoids nozzle clogging when using highly viscous hydrogels or the ubiquitous shear stress affecting cell viability.

While adding microstructural complexity to the constructs is clearly a desirable feature, new challenges arrive with higher complexity. Novel indicators should be developed when evaluating the structure, morphology and functionality of the bioprinted construct. For instance, the IC₅₀ is usually used as a metric for drug response in two-dimensional or monolayer

cultures. Higher values in the case of three-dimensional models are expected since higher dimensionality generates gradients of concentrations of compounds being tested [244]–[246]. However, there is no consensus on how to interpret IC₅₀ for 3D constructs that might inform or be more relevant to understand the biological response to exposure.

D. Multi-Organ Platforms

The biofabrication of the basic functional unit of an organ or tissue as an *in vitro* model confers information about the physiologic or pathologic events that take place in an isolated microenvironment. Unlike *in vivo* models of drug discovery, this differential and remarkable feature proves to be handy when interested in uni- and bi-directional organ-organ crosstalk. However, it is still challenging to evaluate pharmacokinetics (PK) and pharmacodynamics (PD) using *in vitro* methods [247], [248]. Advancements in microfluidics enabled the integration of well-established organ-on-a-chip models [249]–[252] within a single platform interconnected by a network of microchannels to achieve comprehensive organ-organ crosstalk leading to engineered microstructures that resemble systemic behavior. Bioprinting as a complementary technology to manufacture better models of exposure and disease enables automation and spatial resolution of either the entire platform in an uninterrupted one-step fabrication [131] or the bioinspired microarchitectures in the distinct tissue chambers [253].

Thinking about novel viral respiratory threats, an ideal multi-tissue model created using bioprinting techniques, microfluidics and organoids has been proposed [254] to study viral infections including SarS-Cov, MERS-CoV and SarS-CoV-2 [255]. A more conservative approach involves the integration of pre-existing bioprinted and non-bioprinted 3D models of tissues that are affected by the Sars-CoV-2 virus (nasal, lung, cardiovascular, liver, gastrointestinal and renal mucosa) not only to study the pathological infection processes but also to reduce the need for animal models and minimize the timeline for human clinical trials under pandemic conditions [256].

VII. CONCLUSION

This article has detailed the potential of bioprinting to manufacture improved *in vitro* models of exposure and disease by introducing researchers to techniques that include extrusion-, inkjet- and laser-assisted bioprinting. Hydrogels as constituents of bioinks and biomaterial inks gave rise to the versatility offered by this type of technology to design the optimal strategy to recreate microenvironments that represent the physiological and pathophysiological events of organisms *in vivo*. Forty-one bioprinted models were analyzed, including cancer, cardiac, hepatic and skin models that highlight the high cellular viability in the post-bioprinted constructs, the diversity of three-dimensional geometries and the extrusion technique as the most used. Although bioprinting is being adopted as a tool to improve the automation, reproducibility and geometry of *in vitro* models compared to traditional methodologies, it is still a technology that needs to reinforce certain aspects in order to develop advanced models in terms of heterogeneity, microstructural complexity, dynamism and integration capabilities with other models to generate multi-organ platforms where systemic responses need to be evaluated. Altogether, we hope that this survey of the state-of-the-technologies for bioprinting could enhance our

understanding and encourage further developments and implementation of much-needed informative *in vitro* models to study chemical safety, disease progression and exposure responses.

DISCLOSURE

The authors declare that there is no conflict of interest.

REFERENCES

- [1] Center for Devices and Radiological Health, U.S. Food and Drug Administration, "In vitro companion diagnostic devices - Guidance for industry and food and drug administration staff," 2014. Accessed: Sep. 14, 2020. [Online]. Available: <https://www.fda.gov/media/81309/download>
- [2] Official Journal of the European Union L, "Regulation (EU) 2017/746 of the European Parliament and of the Council of 5 April 2017 on in vitro diagnostic medical devices and repealing directive 98/79/EC and Commission decision 2010/227/EU," OJ L 117, May 2017. Accessed: Sep. 14, 2020. [Online]. Available: <https://eur-lex.europa.eu/legal-content/EN/TXT/PDF/?uri=CELEX:32017R0746&from=EN>
- [3] M. Abercrombie, "Ross Granville Harrison, 1870-1959," *Biographical Memoirs Fellows Roy. Soc.*, vol. 7, pp. 110-126, 1961, doi: [10.1098/rsbm.1961.0009](https://doi.org/10.1098/rsbm.1961.0009).
- [4] J. M. Lee et al., "A three-dimensional microenvironment alters protein expression and chemosensitivity of epithelial ovarian cancer cells in vitro," *Lab. Investigation*, vol. 93, no. 5, pp. 528-542, May 2013.
- [5] B. Yao et al., "Biochemical and structural cues of 3D-printed matrix synergistically direct MSC differentiation for functional sweat gland regeneration," *Sci. Adv.*, vol. 6, no. 10, Mar. 2020, Art. no. eaaz1094.
- [6] B. Vagaska, O. Gillham, and P. Ferretti, "Modelling human CNS injury with human neural stem cells in 2- and 3-Dimensional cultures," *Sci. Rep.*, vol. 10, no. 1, Apr. 2020, Art. no. 6785.
- [7] M. Persson et al., "Osteogenic differentiation of human mesenchymal stem cells in a 3D Woven Scaffold," *Sci. Rep.*, vol. 8, no. 1, pp. 1-12, Jul. 2018.
- [8] D. Zujur, K. Kanke, A. C. Lichtler, H. Hojo, U.-I. Chung, and S. Ohba, "Three-dimensional system enabling the maintenance and directed differentiation of pluripotent stem cells under defined conditions," *Sci. Adv.*, vol. 3, no. 5, May 2017, Art. no. e1602875.
- [9] P. DelNero et al., "3D culture broadly regulates tumor cell hypoxia response and angiogenesis via pro-inflammatory pathways," *Biomaterials*, vol. 55, pp. 110-118, Jul. 2015.
- [10] D. Zhang, M. Pekkanen-Mattila, M. Shahsavani, A. Falk, A. I. Teixeira, and A. Herland, "A 3D alzheimer's disease culture model and the induction of P21-activated kinase mediated sensing in iPSC derived neurons," *Biomaterials*, vol. 35, no. 5, pp. 1420-1428, 2014, doi: [10.1016/j.biomaterials.2013.11.028](https://doi.org/10.1016/j.biomaterials.2013.11.028).
- [11] S. Thippabhotla, C. Zhong, and M. He, "3D cell culture stimulates the secretion of in vivo like extracellular vesicles," *Sci. Rep.*, vol. 9, no. 1, Sep. 2019, Art. no. 13012.
- [12] R. J. Klebe, "Cytoscribing: A method for micropositioning cells and the construction of two- and three-dimensional synthetic tissues," *Exp. Cell Res.*, vol. 179, no. 2, pp. 362-373, Dec. 1988.
- [13] A. Atala, "Tissue engineering of human bladder," *Brit. Med. Bull.*, vol. 97, pp. 81-104, 2011.
- [14] W. C. Wilson, W. C. Wilson, and T. Bolland, "Cell and organ printing I: Protein and cell printers," *Anat. Rec.*, vol. 272A, no. 2, pp. 491-496, 2003, doi: [10.1002/ar.a.10057](https://doi.org/10.1002/ar.a.10057).
- [15] K. Jakab, A. Neagu, V. Mironov, R. R. Markwald, and G. Forgacs, "Engineering biological structures of prescribed shape using self-assembling multicellular systems," *Proc. Natl. Acad. Sci. USA*, vol. 101, no. 9, pp. 2864-2869, Mar. 2004.
- [16] K. Karzyński et al., "Use of 3D bioprinting in biomedical engineering for clinical application," *Med. Stud.*, vol. 34, no. 1, pp. 93-97, 2018, doi: [10.5114/ms.2018.74827](https://doi.org/10.5114/ms.2018.74827).
- [17] R. R. Jose, M. J. Rodriguez, T. A. Dixon, F. Omenetto, and D. L. Kaplan, "Evolution of bioinks and additive manufacturing technologies for 3D bioprinting," *ACS Biomater. Sci. Eng.*, vol. 2, no. 10, pp. 1662-1678, 2016, doi: [10.1021/acsbiomaterials.6b00088](https://doi.org/10.1021/acsbiomaterials.6b00088).
- [18] *Standard Terminology for Additive Manufacturing General Principles Terminology*, ISO/ASTM 52900-2015.
- [19] B. Webb and B. J. Doyle, "Parameter optimization for 3D bioprinting of hydrogels," *Bioprinting*, vol. 8, pp. 8-12, 2017, doi: [10.1016/j.bprint.2017.09.001](https://doi.org/10.1016/j.bprint.2017.09.001).
- [20] S.-J. Song, J. Choi, Y.-D. Park, J.-J. Lee, S. Y. Hong, and K. Sun, "A three-dimensional bioprinting system for use with a hydrogel-based biomaterial and printing parameter characterization," *Artif. Organs*, vol. 34, no. 11, pp. 1044-1048, Nov. 2010.
- [21] M. Alruwaili, J. A. Lopez, K. McCarthy, E. G. Reynaud, and B. J. Rodriguez, "Liquid-phase 3D bioprinting of gelatin alginate hydrogels: Influence of printing parameters on hydrogel line width and layer height," *Bio-Des. Manuf.*, vol. 2, no. 3, pp. 172-180, 2019, doi: [10.1007/s42242-019-00043-w](https://doi.org/10.1007/s42242-019-00043-w).
- [22] D. X. B. Chen, *Extrusion Bioprinting of Scaffolds for Tissue Engineering Applications*. Berlin, Germany: Springer, 2019, pp. 117-119, doi: [10.1007/978-3-030-03460-3](https://doi.org/10.1007/978-3-030-03460-3).
- [23] I. T. Ozbolat, *3D Bioprinting: Fundamentals, Principles and Applications*. Cambridge, MA, USA: Academic, 2016, pp. 129-132.
- [24] M. Hospodiu, K. K. Moncal, M. Dey, and I. T. Ozbolat, "Extrusion-Based biofabrication in tissue engineering and regenerative medicine," in *3D in Printing and Biofabrication*. Berlin, Germany: Springer, 2016, pp. 1-27, doi: [10.1007/978-3-319-40498-1_10-1](https://doi.org/10.1007/978-3-319-40498-1_10-1).
- [25] S. Khalil, J. Nam, and W. Sun, "Multi-nozzle deposition for construction of 3D biopolymer tissue scaffolds," *Rapid Prototyping J.*, vol. 11, no. 1, pp. 9-17, 2005, doi: [10.1108/13552540510573347](https://doi.org/10.1108/13552540510573347).
- [26] R. Chang, J. Nam, and W. Sun, "Effects of dispensing pressure and nozzle diameter on cell survival from solid freeform fabrication-based direct cell writing," *Tissue Eng. Part A*, vol. 14, no. 1, pp. 41-48, Jan. 2008.
- [27] C. M. Smith, J. J. Christian, W. L. Warren, and S. K. Williams, "Characterizing environmental factors that impact the viability of tissue-engineered constructs fabricated by a direct-write bioassembly tool," *Tissue Eng.*, vol. 13, no. 2, pp. 373-383, Feb. 2007.
- [28] W. Lee et al., "On-demand three-dimensional freeform fabrication of multi-layered hydrogel scaffold with fluidic channels," *Biotechnol. Bioeng.*, vol. 105, no. 6, pp. 1178-1186, Apr. 2010.
- [29] A. Faulkner-Jones, S. Greenhough, J. A. King, J. Gardner, A. Courtney, and W. Shu, "Development of a valve-based cell printer for the formation of human embryonic stem cell spheroid aggregates," *Biofabrication*, vol. 5, no. 1, Mar. 2013, Art. no. 015013.
- [30] J. Visser et al., "Biofabrication of multi-material anatomically shaped tissue constructs," *Biofabrication*, vol. 5, no. 3, Sep. 2013, Art. no. 035007.
- [31] L. Ning et al., "Process-induced cell damage: Pneumatic versus screw-driven bioprinting," *Biofabrication*, vol. 12, no. 2, 2020, Art. no. 025011, doi: [10.1088/1758-5090/ab5f53](https://doi.org/10.1088/1758-5090/ab5f53).
- [32] J. Bohandy, B. F. Kim, and F. J. Adrian, "Metal deposition from a supported metal film using an excimer laser," *J. Appl. Phys.*, vol. 60, no. 4, pp. 1538-1539, 1986, doi: [10.1063/1.337287](https://doi.org/10.1063/1.337287).
- [33] F. J. Adrian, J. Bohandy, B. F. Kim, A. N. Jette, and P. Thompson, "A study of the mechanism of metal deposition by the laser-induced forward transfer process," *J. Vac. Sci. Technol. B: Microelectron. Nanometer Struct.*, vol. 5, no. 5, 1987, Art. no. 1490, doi: [10.1116/1.583661](https://doi.org/10.1116/1.583661).
- [34] M. Morales, D. Munoz-Martin, A. Marquez, S. Lauzurica, and C. Molpeceres, "Laser-Induced forward transfer techniques and applications," in *Proc. Int. Conf. Laser Mater. Process.*, 2018, pp. 339-379, doi: [10.1016/b978-0-08-101252-9.00013-3](https://doi.org/10.1016/b978-0-08-101252-9.00013-3).
- [35] S. Catros, V. Keriquel, J.-C. Fricain, and F. Guillemot, "In vivo and in situ biofabrication by laser-assisted bioprinting," in *Essentials of 3D Biofabrication and Translation*. Berlin, Germany: Springer, 2015, pp. 81-87, doi: [10.1016/b978-0-12-800972-7.00005-0](https://doi.org/10.1016/b978-0-12-800972-7.00005-0).
- [36] M. Ali, E. Pages, A. Ducom, A. Fontaine, and F. Guillemot, "Controlling laser-induced jet formation for bioprinting mesenchymal stem cells with high viability and high resolution," *Biofabrication*, vol. 6, no. 4, Sep. 2014, Art. no. 045001.
- [37] B. Taidi, G. Lebernede, L. Koch, P. Perre, and B. Chichkov, "Colony development of laser printed eukaryotic (yeast and microalga) microorganisms in co-culture," *Int. J. Bioprinting*, vol. 2, no. 2, 2016, doi: [10.18063/ijb.2016.02.001](https://doi.org/10.18063/ijb.2016.02.001).
- [38] C. M. Othon, X. Wu, J. J. Anders, and B. R. Ringeisen, "Single-cell printing to form three-dimensional lines of olfactory ensheathing cells," *Biomed. Mater.*, vol. 3, no. 3, Sep. 2008, Art. no. 034101.
- [39] L. Koch, O. Brandt, A. Deiwick, and B. Chichkov, "Laser assisted bioprinting at different wavelengths and pulse durations with a metal dynamic release layer: A parametric study," *Int. J. Bioprinting*, vol. 3, no. 1, 2017, Art. no. 1, doi: [10.18063/ijb.2017.01.001](https://doi.org/10.18063/ijb.2017.01.001).
- [40] A. Sorkio et al., "Human stem cell based corneal tissue mimicking structures using laser-assisted 3D bioprinting and functional bioinks," *Biomaterials*, vol. 171, pp. 57-71, Jul. 2018.

- [41] F. Kawecki, W. P. Clafshenkel, F. A. Auger, J.-M. Bourget, J. Fradette, and R. Devillard, "Self-assembled human osseous cell sheets as living biopapers for the laser-assisted bioprinting of human endothelial cells," *Biofabrication*, vol. 10, no. 3, Apr. 2018, Art. no. 035006.
- [42] B. Guillotin *et al.*, "Laser assisted bioprinting of engineered tissue with high cell density and microscale organization," *Biomaterials*, vol. 31, no. 28, pp. 7250–7256, Oct. 2010.
- [43] B. Guillotin *et al.*, *Biofabrication: Chapter 6. Laser-Assisted Bioprinting For Tissue Engineering*. Amsterdam, The Netherlands: Elsevier, 2013, pp. 98–101.
- [44] H. Gudapati, M. Dey, and I. Ozbolat, "A comprehensive review on droplet-based bioprinting: Past, present and future," *Biomaterials*, vol. 102, pp. 20–42, Sep. 2016.
- [45] L. Rayleigh, "On the instability of jets," *London Math. Soc.*, vol. 1, pp. 4–13, 1878.
- [46] D. Wu and C. Xu, "Predictive modeling of droplet formation processes in inkjet-based bioprinting," *J. Manuf. Sci. Eng.*, vol. 140, no. 10, 2018, Art. no. 101007, doi: [10.1115/1.4040619](https://doi.org/10.1115/1.4040619).
- [47] D. Wu, C. Xu, and S. Krishnamoorthy, "Predictive modeling of droplet velocity and size in inkjet-based bioprinting," in *Proc. Manuf. Equip. Syst.*, 2018, pp. 1–6, doi: [10.1115/msec2018-6513](https://doi.org/10.1115/msec2018-6513).
- [48] J. Shi, J. Song, B. Song, and W. F. Lu, "Multi-objective optimization design through machine learning for drop-on-demand bioprinting," *Engineering*, vol. 5, no. 3, pp. 586–593, 2019, doi: [10.1016/j.eng.2018.12.009](https://doi.org/10.1016/j.eng.2018.12.009).
- [49] H. Wijshoff, "The dynamics of the piezo inkjet printhead operation☆," *Phys. Rep.*, vol. 491, no. 4–5, pp. 77–177, 2010, doi: [10.1016/j.physrep.2010.03.003](https://doi.org/10.1016/j.physrep.2010.03.003).
- [50] X. Cui and T. Boland, "Human microvasculature fabrication using thermal inkjet printing technology," *Biomaterials*, vol. 30, no. 31, pp. 6221–6227, Oct. 2009.
- [51] E. A. Roth, T. Xu, M. Das, C. Gregory, J. J. Hickman, and T. Boland, "Inkjet printing for high-throughput cell patterning," *Biomaterials*, vol. 25, no. 17, pp. 3707–3715, Aug. 2004.
- [52] T. Xu *et al.*, "Construction of high-density bacterial colony arrays and patterns by the ink-jet method," *Biotechnol. Bioeng.*, vol. 85, no. 1, pp. 29–33, Jan. 2004.
- [53] X. Cui, D. Dean, Z. M. Ruggeri, and T. Boland, "Cell damage evaluation of thermal inkjet printed Chinese hamster ovary cells," *Biotechnol. Bioeng.*, vol. 106, no. 6, pp. 963–969, Aug. 2010.
- [54] S. Hewes, A. D. Wong, and P. C. Searson, "Bioprinting microvessels using an inkjet printer," *Bioprinting*, vol. 7, pp. 14–18, 2017, doi: [10.1016/j.bprint.2017.05.002](https://doi.org/10.1016/j.bprint.2017.05.002).
- [55] X. Ma *et al.*, "Deterministically patterned biomimetic human iPSC-derived hepatic model via rapid 3D bioprinting," *Proc. Natl. Acad. Sci. USA*, vol. 113, no. 8, pp. 2206–2211, Feb. 2016.
- [56] K. L. Miller *et al.*, "Rapid 3D bioprinting of a human iPSC-derived cardiac micro-tissue for high-throughput drug testing," *Organs-a-Chip*, vol. 3, 2021, Art. no. 100007, doi: [10.1016/j.ooc.2021.100007](https://doi.org/10.1016/j.ooc.2021.100007).
- [57] S. Abdollahi, J. Boktor, and N. Hibino, "Bioprinting of freestanding vascular grafts and the regulatory considerations for additively manufactured vascular prostheses," *Transl. Res.*, vol. 211, pp. 123–138, Sep. 2019.
- [58] J. M. Shapiro, B. W. Drinkwater, A. W. Perriman, and M. Fraser, "Sonolithography: In-air ultrasonic particulate and droplet manipulation for multiscale surface patterning," *Adv. Mater. Technol.*, vol. 6, no. 3, 2021, Art. no. 2000689, doi: [10.1002/admt.202000689](https://doi.org/10.1002/admt.202000689).
- [59] B. Ayan *et al.*, "Aspiration-assisted bioprinting for precise positioning of biologics," *Sci. Adv.*, vol. 6, no. 10, Mar. 2020, Art. no. eaaw5111.
- [60] N. I. Moldovan, N. Hibino, and K. Nakayama, "Principles of the Kenzan method for robotic cell spheroid-based three-dimensional Bioprinting," *Tissue Eng. Part B Rev.*, vol. 23, no. 3, pp. 237–244, Jun. 2017.
- [61] P. N. Bernal *et al.*, "Volumetric bioprinting of complex living-tissue constructs within seconds," *Adv. Mater.*, vol. 31, no. 42, Oct. 2019, Art. no. e1904209.
- [62] J. Groll *et al.*, "A definition of bioinks and their distinction from biomaterial inks," *Biofabrication*, vol. 11, no. 1, Nov. 2018, Art. no. 013001.
- [63] N. A. Peppas, J. Z. Hilt, A. Khademhosseini, and R. Langer, "Hydrogels in biology and medicine: From molecular principles to biotechnology," *Adv. Mater.*, vol. 18, no. 11, pp. 1345–1360, 2006, doi: [10.1002/adma.200501612](https://doi.org/10.1002/adma.200501612).
- [64] N. Annabi *et al.*, "25th anniversary article: Rational design and applications of hydrogels in regenerative medicine," *Adv. Mater.*, vol. 26, no. 1, pp. 85–123, Jan. 2014.
- [65] C. K. Chua and W. Y. Yeong, *Bioprinting*. Singapore: World Scientific, 2015, p. 129.
- [66] L. Ouyang, C. B. Highley, W. Sun, and J. A. Burdick, "A generalizable strategy for the 3D bioprinting of hydrogels from nonviscous Photo-crosslinkable inks," *Adv. Mater.*, vol. 29, no. 8, Feb. 2017, Art. no. 1604983, doi: [10.1002/adma.201604983](https://doi.org/10.1002/adma.201604983).
- [67] J. Hazur *et al.*, "Improving alginate printability for biofabrication: Establishment of a universal and homogeneous pre-crosslinking technique," *Biofabrication*, vol. 12, no. 4, Jul. 2020, Art. no. 045004.
- [68] M. L. Jia, E. T. Sheng, Z. Zhu, and Y. Y. Wai, "Biomaterials for bioprinting," in *3D in Bioprinting and Nanotechnology in Tissue Engineering and Regenerative Medicine*. Cambridge, MA, USA: Academic, 2015, pp. 129–148.
- [69] E. O. Osidak, V. I. Kozhukhov, M. S. Osidak, and S. P. Domogatskiy, "Collagen as bioink for bioprinting: A comprehensive review," *Int. J. Bioprinting*, vol. 6, no. 3, 2020, Art. no. 270, doi: [10.18063/ijb.v6i3.270](https://doi.org/10.18063/ijb.v6i3.270).
- [70] A. K. Lynn, I. V. Yannas, and W. Bonfield, "Antigenicity and immunogenicity of collagen," *J. Biomed. Mater. Res. B Appl. Biomater.*, vol. 71, no. 2, pp. 343–354, Nov. 2004.
- [71] J.-L. Pariente, B.-S. Kim, and A. Atala, "In vitro biocompatibility evaluation of naturally derived and synthetic biomaterials using normal human bladder smooth muscle cells," *J. Urol.*, vol. 167, no. 4, pp. 1867–1871, Apr. 2002.
- [72] T. K. Merceron and S. V. Murphy, "Hydrogels for 3D bioprinting applications," in *Essentials of 3D Biofabrication and Translation*. Amsterdam, Netherlands: Elsevier, 2015, pp. 249–270, doi: [10.1016/b978-0-12-800972-7.00014-1](https://doi.org/10.1016/b978-0-12-800972-7.00014-1).
- [73] M. Hospodiuk, M. Dey, D. Sosnoski, and I. T. Ozbolat, "The bioink: A comprehensive review on bioprintable materials," *Biotechnol. Adv.*, vol. 35, no. 2, pp. 217–239, Mar. 2017.
- [74] D. Zhou, J. Chen, B. Liu, X. Zhang, X. Li, and T. Xu, "Bioinks for jet-based bioprinting," *Bioprinting*, vol. 16, 2019, Art. no. e00060, doi: [10.1016/j.bprint.2019.e00060](https://doi.org/10.1016/j.bprint.2019.e00060).
- [75] K. Y. Lee and D. J. Mooney, "Alginate: Properties and biomedical applications," *Prog. Polym. Sci.*, vol. 37, no. 1, pp. 106–126, 2012, doi: [10.1016/j.progpolymsci.2011.06.003](https://doi.org/10.1016/j.progpolymsci.2011.06.003).
- [76] I. Donati, S. Holtan, Y. A. Mørch, M. Borgogna, M. Dentini, and G. Skjåk-Braek, "New hypothesis on the role of alternating sequences in calcium-alginate gels," *Biomacromolecules*, vol. 6, no. 2, pp. 1031–1040, Mar. 2005.
- [77] J. L. Drury, R. G. Dennis, and D. J. Mooney, "The tensile properties of alginate hydrogels," *Biomaterials*, vol. 25, no. 16, pp. 3187–3199, 2004, doi: [10.1016/j.biomaterials.2003.10.002](https://doi.org/10.1016/j.biomaterials.2003.10.002).
- [78] L. Ning, N. Zhu, F. Mohabatpour, M. D. Sarker, D. J. Schreyer, and X. Chen, "Bioprinting Schwann cell-laden scaffolds from low-viscosity hydrogel compositions," *J. Mater. Chem. B*, vol. 7, no. 29, pp. 4538–4551, 2019, doi: [10.1039/c9tb00669a](https://doi.org/10.1039/c9tb00669a).
- [79] G. F. Acosta-Vélez, C. S. Linsley, M. C. Craig, and B. M. Wu, "Photocurable bioink for the inkjet 3D pharming of hydrophilic drugs," *Bioeng. (Basel)*, vol. 4, no. 1, Jan. 2017, Art. no. 11, doi: [10.3390/bioengineering4010011](https://doi.org/10.3390/bioengineering4010011).
- [80] M. T. Poldervaart *et al.*, "3D bioprinting of methacrylated hyaluronic acid (MeHA) hydrogel with intrinsic osteogenicity," *PLoS One*, vol. 12, no. 6, Jun. 2017, Art. no. e0177628.
- [81] S. Wu, R. Xu, B. Duan, and P. Jiang, "Three-Dimensional hyaluronic acid hydrogel-based models for in vitro human iPSC-Derived NPC culture and differentiation," *J. Mater. Chem. B Mater. Biol. Med.*, vol. 5, no. 21, pp. 3870–3878, Jun. 2017.
- [82] C. Antich *et al.*, "Bio-inspired hydrogel composed of hyaluronic acid and alginate as a potential bioink for 3D bioprinting of articular cartilage engineering constructs," *Acta Biomater.*, vol. 106, pp. 114–123, Apr. 2020.
- [83] S. Sakai, H. Ohi, T. Hotta, H. Kamei, and M. Taya, "Differentiation potential of human adipose stem cells bioprinted with hyaluronic acid/gelatin-based bioink through microextrusion and visible light-initiated crosslinking," *Biopolymers*, vol. 109, no. 2, 2018, Art. no. e23080, doi: [10.1002/bip.23080](https://doi.org/10.1002/bip.23080).
- [84] N. Law *et al.*, "Characterisation of hyaluronic acid methylcellulose hydrogels for 3D bioprinting," *J. Mech. Behav. Biomed. Mater.*, vol. 77, pp. 389–399, 2018, doi: [10.1016/j.jmbm.2017.09.031](https://doi.org/10.1016/j.jmbm.2017.09.031).
- [85] A. Skardal *et al.*, "A hydrogel bioink toolkit for mimicking native tissue biochemical and mechanical properties in bioprinted tissue constructs," *Acta Biomater.*, vol. 25, pp. 24–34, Oct. 2015.
- [86] A. Skardal *et al.*, "Bioprinting cellularized constructs using a Tissue-specific hydrogel bioink," *J. Visualized Experiments*, vol. 21, no. 110, 2016, Art. no. e53606, doi: [10.3791/53606](https://doi.org/10.3791/53606).

- [87] A. Mazzocchi, M. Devarasetty, R. Huntwork, S. Soker, and A. Skardal, "Optimization of collagen type I-hyaluronan hybrid bioink for 3D bioprinted liver microenvironments," *Biofabrication*, vol. 11, no. 1, Oct. 2018, Art. no. 015003.
- [88] S. Zhao et al., "Bio-functionalized silk hydrogel microfluidic systems," *Biomaterials*, vol. 93, pp. 60–70, Jul. 2016.
- [89] V. K. Lee et al., "Creating perfused functional vascular channels using 3D bio-printing technology," *Biomaterials*, vol. 35, no. 28, pp. 8092–8102, Sep. 2014.
- [90] A. Bigi, G. Cojazzi, S. Panzavolta, K. Rubini, and N. Roveri, "Mechanical and thermal properties of gelatin films at different degrees of glutaraldehyde crosslinking," *Biomaterials*, vol. 22, no. 8, pp. 763–768, Apr. 2001.
- [91] H. W. Sun, R. J. Feigal, and H. H. Messer, "Cytotoxicity of glutaraldehyde and formaldehyde in relation to time of exposure and concentration," *Pediatr. Dent.*, vol. 12, no. 5, pp. 303–307, Sep. 1990.
- [92] P. Occhetta, R. Visone, L. Russo, L. Cipolla, M. Moretti, and M. Rasponi, "VA-086 methacrylate gelatine photopolymerizable hydrogels: A parametric study for highly biocompatible 3D cell embedding," *J. Biomed. Mater. Res. A*, vol. 103, no. 6, pp. 2109–2117, Jun. 2015.
- [93] A. I. Van Den Bulcke, B. Bogdanov, N. De Rooze, E. H. Schacht, M. Cornelissen, and H. Berghmans, "Structural and rheological properties of methacrylamide modified gelatin hydrogels," *Biomacromolecules*, vol. 1, no. 1, pp. 31–38, Spring 2000.
- [94] E. Hoch, T. Hirth, G. E. M. Tovar, and K. Borchers, "Chemical tailoring of gelatin to adjust its chemical and physical properties for functional bioprinting," *J. Mater. Chem. B*, vol. 1, no. 41, 2013, Art. no. 5675, doi: [10.1039/c3tb20745e](https://doi.org/10.1039/c3tb20745e).
- [95] M. L. Schwartz, S. V. Pizzo, R. L. Hill, and P. A. McKee, "Human factor XIII from plasma and platelets. Molecular weights, subunit structures, proteolytic activation, and cross-linking of fibrinogen and fibrin," *J. Biol. Chem.*, vol. 248, no. 4, pp. 1395–1407, Feb. 1973.
- [96] M. Robinson, S. Douglas, and S. M. Willerth, "Mechanically stable fibrin scaffolds promote viability and induce neurite outgrowth in neural aggregates derived from human induced pluripotent stem cells," *Sci. Rep.*, vol. 7, no. 1, Jul. 2017, Art. no. 6250.
- [97] R. M. Schek, A. J. Michalek, and J. C. Iatridis, "Genipin-crosslinked fibrin hydrogels as a potential adhesive to augment intervertebral disc annulus repair," *Eur. Cell. Mater.*, vol. 21, pp. 373–383, Apr. 2011.
- [98] R. M. Irwin et al., "The clot thickens: Autologous and allogeneic fibrin sealants are mechanically equivalent in an ex vivo model of cartilage repair," *Plos One*, vol. 14, no. 11, 2019, Art. no. e0224756, doi: [10.1371/journal.pone.0224756](https://doi.org/10.1371/journal.pone.0224756).
- [99] W. L. Ng, J. M. Lee, M. Zhou, and W. Y. Yeong, "Hydrogels for 3-D bioprinting-based tissue engineering," *Rapid Prototyping Biomaterials*, vol. 2020, pp. 183–204, 2020, doi: [10.1016/b978-0-08-102663-2.00008-3](https://doi.org/10.1016/b978-0-08-102663-2.00008-3).
- [100] S. L. Rowe, S. Lee, and J. P. Stegmann, "Influence of thrombin concentration on the mechanical and morphological properties of cell-seeded fibrin hydrogels," *Acta Biomater.*, vol. 3, no. 1, pp. 59–67, Jan. 2007.
- [101] K. B. Bjugstad, D. E. Redmond Jr, K. J. Lampe, D. S. Kern, J. R. Sladek Jr, and M. J. Mahoney, "Biocompatibility of PEG-based hydrogels in primate brain," *Cell Transplant*, vol. 17, no. 4, pp. 409–415, 2008.
- [102] J. Wang, F. Zhang, W. P. Tsang, C. Wan, and C. Wu, "Fabrication of injectable high strength hydrogel based on 4-arm star PEG for cartilage tissue engineering," *Biomaterials*, vol. 120, pp. 11–21, Mar. 2017.
- [103] H. Y. Cho et al., "Synthesis of biocompatible PEG-Based star polymers with cationic and degradable core for siRNA delivery," *Biomacromolecules*, vol. 12, no. 10, pp. 3478–3486, Oct. 2011.
- [104] C.-C. Lin, "Recent advances in crosslinking chemistry of biomimetic poly(ethylene glycol) hydrogels," *RSC Adv.*, vol. 5, no. 50, pp. 39844–398583, Jan. 2015.
- [105] M. Parlato, S. Reichert, N. Barney, and W. L. Murphy, "Poly(ethylene glycol) hydrogels with adaptable mechanical and degradation properties for use in biomedical applications," *Macromol. Biosci.*, vol. 14, no. 5, pp. 687–698, May 2014.
- [106] J. Lee, H. Lee, and J. Andrade, "Blood compatibility of polyethylene oxide surfaces," *Prog. Polym. Sci.*, vol. 20, no. 6, pp. 1043–1079, 1995, doi: [10.1016/0079-6700\(95\)00011-4](https://doi.org/10.1016/0079-6700(95)00011-4).
- [107] T. H. Barker, G. M. Fuller, M. M. Klinger, D. S. Feldman, and J. S. Hagood, "Modification of fibrinogen with poly(ethylene glycol) and its effects on fibrin clot characteristics," *J. Biomed. Mater. Res.*, vol. 56, no. 4, pp. 529–535, Sep. 2001.
- [108] B. V. Sridhar, J. L. Brock, J. S. Silver, J. L. Leight, M. A. Randolph, and K. S. Anseth, "Development of a cellularly degradable PEG hydrogel to promote articular cartilage extracellular matrix deposition," *Adv. Healthc. Mater.*, vol. 4, no. 5, pp. 702–713, Apr. 2015.
- [109] N. Cohen et al., "Cell encapsulation utilizing PEG-fibrinogen hydrogel supports viability and enhances productivity under stress conditions," *Cytotechnology*, vol. 70, no. 3, pp. 1075–1083, Jun. 2018.
- [110] H. Wang et al., "Assembly of RGD-Modified hydrogel micromodules into permeable three-dimensional hollow microtissues mimicking in vivo tissue structures," *ACS Appl. Mater. Interfaces*, vol. 9, no. 48, pp. 41669–41679, Dec. 2017.
- [111] G. Gao, T. Yonezawa, K. Hubbell, G. Dai, and X. Cui, "Inkjet-bioprinted acrylated peptides and PEG hydrogel with human mesenchymal stem cells promote robust bone and cartilage formation with minimal printhead clogging," *Biotechnol. J.*, vol. 10, no. 10, pp. 1568–1577, Oct. 2015.
- [112] G. Gao et al., "Improved properties of bone and cartilage tissue from 3D inkjet-bioprinted human mesenchymal stem cells by simultaneous deposition and photocrosslinking in PEG-GelMA," *Biotechnol. Lett.*, vol. 37, no. 11, pp. 2349–2355, Nov. 2015.
- [113] M. Managa, J. Britton, E. Prinsloo, and T. Nyokong, "Effects of pluronic F127 micelles as delivering agents on the vitro dark toxicity and photodynamic therapy activity of carboxy and pyrene substituted porphyrins," *Polyhedron*, vol. 152, pp. 102–107, 2018, doi: [10.1016/j.poly.2018.06.031](https://doi.org/10.1016/j.poly.2018.06.031).
- [114] D. V. C. Mendonça et al., "Poloxamer 407 (Pluronic F127)-based polymeric micelles for amphotericin B: In vitro biological activity, toxicity and in vivo therapeutic efficacy against murine tegumentary leishmaniasis," *Exp. Parasitol.*, vol. 169, pp. 34–42, 2016, doi: [10.1016/j.exppara.2016.07.005](https://doi.org/10.1016/j.exppara.2016.07.005).
- [115] Y. S. Zhang et al., "Bioprinted thrombosis-on-a-chip," *Lab Chip*, vol. 16, no. 21, pp. 4097–4105, Oct. 2016.
- [116] M. Müller, J. Becher, M. Schnabelrauch, and M. Zenobi-Wong, "Nanos-structured pluronic hydrogels as bioinks for 3D bioprinting," *Biofabrication*, vol. 7, no. 3, Aug. 2015, Art. no. 035006.
- [117] Y. Xu, Y. Hu, C. Liu, H. Yao, B. Liu, and S. Mi, "A novel strategy for creating tissue-engineered biomimetic blood vessels using 3D bioprinting technology," *Materials*, vol. 11, no. 9, 2018, Art. no. 1581, doi: [10.3390/ma11091581](https://doi.org/10.3390/ma11091581).
- [118] H. Geng, H. Song, J. Qi, and D. Cui, "Sustained release of VEGF from PLGA nanoparticles embedded thermo-sensitive hydrogel in full-thickness porcine bladder acellular matrix," *Nanoscale Res. Lett.*, vol. 6, no. 1, Apr. 2011, Art. no. 312.
- [119] J. J. Escobar-Chávez, M. López-Cervantes, A. Naik, Y. N. Kalia, D. Quintanar-Guerrero, and A. Ganem-Quintanar, "Applications of thermo-reversible pluronic F-127 gels in pharmaceutical formulations," *J. Pharm. Pharm. Sci.*, vol. 9, no. 3, pp. 339–358, 2006.
- [120] R. Suntornnond, E. Y. S. Tan, J. An, and C. K. Chua, "A highly printable and biocompatible hydrogel composite for direct printing of soft and perfusable vasculature-like structures," *Sci. Rep.*, vol. 7, no. 1, Dec. 2017, Art. no. 16902.
- [121] H.-W. Kang, S. J. Lee, I. K. Ko, C. Kengla, J. J. Yoo, and A. Atala, "A 3D bioprinting system to produce human-scale tissue constructs with structural integrity," *Nature Biotechnol.*, vol. 34, no. 3, pp. 312–319, Mar. 2016.
- [122] A. Banks, X. Guo, J. Chen, S. Kumpaty, and W. Zhang, "Novel bioprinting method using a pectin based bioink," *Technol. Health Care*, vol. 25, no. 4, pp. 651–655, 2017, doi: [10.3233/thc-160764](https://doi.org/10.3233/thc-160764).
- [123] S. Peng, J.-Y. Lin, M.-H. Cheng, C.-W. Wu, and I.-M. Chu, "A cell-compatible PEO-PPO-PEO (Pluronic)-based hydrogel stabilized through secondary structures," *Mater. Sci. Eng.: C*, vol. 69, pp. 421–428, 2016, doi: [10.1016/j.msec.2016.06.091](https://doi.org/10.1016/j.msec.2016.06.091).
- [124] H. Lee et al., "Chondrocyte 3D-culture in RGD-modified crosslinked hydrogel with temperature-controllable modulus," *Macromol. Res.*, vol. 20, no. 1, pp. 106–111, 2012, doi: [10.1007/s13233-012-0074-6](https://doi.org/10.1007/s13233-012-0074-6).
- [125] E. Gioffredi et al., "Pluronic F127 hydrogel characterization and biofabrication in cellularized constructs for tissue engineering applications," *Procedia CIRP*, vol. 49, pp. 125–132, 2016, doi: [10.1016/j.procir.2015.11.001](https://doi.org/10.1016/j.procir.2015.11.001).
- [126] S. T. Bendtsen, S. P. Quinnell, and M. Wei, "Development of a novel alginate-polyvinyl alcohol-hydroxyapatite hydrogel for 3D bioprinting bone tissue engineered scaffolds," *J. Biomed. Mater. Res. A*, vol. 105, no. 5, pp. 1457–1468, May 2017.
- [127] J. Park et al., "Cell-laden 3D bioprinting hydrogel matrix depending on different compositions for soft tissue engineering: Characterization and evaluation," *Mater. Sci. Eng. C Mater. Biol. Appl.*, vol. 71, pp. 678–684, Feb. 2017.

- [128] N. Cao, X. B. Chen, and D. J. Schreyer, "Influence of calcium ions on cell survival and proliferation in the context of an alginate hydrogel," *ISRN Chem. Eng.*, vol. 2012, pp. 1–9, 2012, doi: [10.5402/2012/516461](https://doi.org/10.5402/2012/516461).
- [129] Y. Zhao, Y. Li, S. Mao, W. Sun, and R. Yao, "The influence of printing parameters on cell survival rate and printability in microextrusion-based 3D cell printing technology," *Biofabrication*, vol. 7, no. 4, Nov. 2015, Art. no. 045002.
- [130] A. Blaeser, D. F. Duarte Campos, U. Puster, W. Richtering, M. M. Stevens, and H. Fischer, "Controlling shear stress in 3D bioprinting is a key factor to balance printing resolution and stem cell integrity," *Adv. Healthc. Mater.*, vol. 5, no. 3, pp. 326–333, Feb. 2016.
- [131] H. Lee and D.-W. Cho, "One-step fabrication of an organ-on-a-chip with spatial heterogeneity using a 3D bioprinting technology," *Lab Chip*, vol. 16, no. 14, pp. 2618–2625, Jul. 2016.
- [132] B. S. Kim, J.-S. Lee, G. Gao, and D.-W. Cho, "Direct 3D cell-printing of human skin with functional transwell system," *Biofabrication*, vol. 9, no. 2, Jun. 2017, Art. no. 025034.
- [133] S. Ramasamy *et al.*, "Optimized construction of a full thickness human skin equivalent using 3D bioprinting and a PCL/collagen dermal scaffold," *Bioprinting*, vol. 21, 2021, Art. no. e00123, doi: [10.1016/j.bprint.2020.e00123](https://doi.org/10.1016/j.bprint.2020.e00123).
- [134] K. Hölzl, S. Lin, L. Tytgat, S. Van Vlierberghe, L. Gu, and A. Ovsianikov, "Bioink properties before, during and after 3D bioprinting," *Biofabrication*, vol. 8, no. 3, 2016, Art. no. 032002, doi: [10.1088/1758-5090/8/3/032002](https://doi.org/10.1088/1758-5090/8/3/032002).
- [135] S. V. Murphy and A. Atala, "3D bioprinting of tissues and organs," *Nature Biotechnol.*, vol. 32, no. 8, pp. 773–785, 2014, doi: [10.1038/nbt.2958](https://doi.org/10.1038/nbt.2958).
- [136] N. Paxton, W. Smolan, T. Böck, F. Melchels, J. Groll, and T. Jungst, "Proposal to assess printability of bioinks for extrusion-based bioprinting and evaluation of rheological properties governing bioprintability," *Biofabrication*, vol. 9, no. 4, Nov. 2017, Art. no. 044107.
- [137] N. Diamantides, C. Dugopolski, E. Blahut, S. Kennedy, and L. J. Bonassar, "High density cell seeding affects the rheology and printability of collagen bioinks," *Biofabrication*, vol. 11, no. 4, Aug. 2019, Art. no. 045016.
- [138] W. Liu *et al.*, "Extrusion bioprinting of shear-thinning gelatin methacryloyl bioinks," *Adv. Healthc. Mater.*, vol. 6, Jun. 2017, Art. no. 12, doi: [10.1002/adhm.201601451](https://doi.org/10.1002/adhm.201601451).
- [139] J. Malda *et al.*, "25th anniversary article: Engineering hydrogels for biofabrication," *Adv. Mater.*, vol. 25, no. 36, pp. 5011–5028, Sep. 2013.
- [140] M. Guvendiren, H. D. Lu, and J. A. Burdick, "Shear-thinning hydrogels for biomedical applications," *Soft Matter*, vol. 8, no. 2, pp. 260–272, 2012, doi: [10.1039/c1sm06513k](https://doi.org/10.1039/c1sm06513k).
- [141] S. Uman, A. Dhand, and J. A. Burdick, "Recent advances in shear-thinning and self-healing hydrogels for biomedical applications," *J. Appl. Polym. Sci.*, vol. 137, 2019, Art. no. 48668, doi: [10.1002/app.48668](https://doi.org/10.1002/app.48668).
- [142] R. Dorey, *Ceramic Thick Films For MEMS and Microdevices*. Amsterdam, Netherlands: Elsevier, 2012, pp. 70–73, doi: [10.1016/c2009-0-20338-2](https://doi.org/10.1016/c2009-0-20338-2).
- [143] I. T. Norton, F. Spyropoulos, and P. Cox, *Practical Food Rheology: An Interpretive Approach*. Hoboken, NJ, USA: Wiley, 2010, p. 14.
- [144] A. Jobling and J. Roberts, "Rheology of disperse systems," *Nature*, vol. 180, no. 4593, pp. 957–959, 1957, doi: [10.1038/180957a0](https://doi.org/10.1038/180957a0).
- [145] R. Wei *et al.*, "Bidirectionally pH-Responsive zwitterionic polymer hydrogels with switchable selective adsorption capacities for anionic and cationic dyes," *Ind. Eng. Chem. Res.*, vol. 57, no. 24, pp. 8209–8219, 2018, doi: [10.1021/acs.iecr.8b01027](https://doi.org/10.1021/acs.iecr.8b01027).
- [146] L. Brannon-Peppas and N. A. Peppas, "Equilibrium swelling behavior of pH-sensitive hydrogels," *Chem. Eng. Sci.*, vol. 46, no. 3, pp. 715–722, 1991, doi: [10.1016/0009-2509\(91\)80177-z](https://doi.org/10.1016/0009-2509(91)80177-z).
- [147] H. Chamkouri, "A review of hydrogels, their properties and applications in medicine," *Amer. J. Biomed. Sci. Res.*, vol. 11, no. 6, pp. 485–493, 2021, doi: [10.34297/ajbsr.2021.11.001682](https://doi.org/10.34297/ajbsr.2021.11.001682).
- [148] L. Klouda, "Thermoresponsive hydrogels in biomedical applications: A seven-year update," *Eur. J. Pharm. Biopharm.*, vol. 97, no. Pt B, pp. 338–349, Nov. 2015.
- [149] J. M. G. Swann, W. Bras, P. D. Topham, J. R. Howse, and A. J. Ryan, "Effect of the hofmeister anions upon the swelling of a self-assembled pH-responsive hydrogel," *Langmuir*, vol. 26, no. 12, pp. 10191–10197, Jun. 2010.
- [150] M. Jaspers, A. E. Rowan, and P. H. J. Kouwer, "Tuning hydrogel mechanics using the hofmeister effect," *Adv. Funct. Mater.*, vol. 25, no. 41, pp. 6503–6510, 2015, doi: [10.1002/adfm.201502241](https://doi.org/10.1002/adfm.201502241).
- [151] H. Holback, Y. Yeo, and K. Park, "Hydrogel swelling behavior and its biomedical applications," *Biomed. Hydrogels*, pp. 3–24, 2011, doi: [10.1533/9780857091383.1.3](https://doi.org/10.1533/9780857091383.1.3).
- [152] M. A. Malana, R. Zohra, and M. S. Khan, "Rheological characterization of novel physically crosslinked terpolymeric hydrogels at different temperatures," *Korea-Aust. Rheol. J.*, vol. 24, no. 3, pp. 155–162, 2012, doi: [10.1007/s13367-012-0019-9](https://doi.org/10.1007/s13367-012-0019-9).
- [153] F. Kousar, M. A. Malana, A. H. Chughtai, and M. S. Khan, "Synthesis and characterization of methacrylamide-acrylic acid-N-isopropylacrylamide polymeric hydrogel: Degradation kinetics and rheological studies," *Polym. Bull.*, vol. 75, no. 3, pp. 1275–1298, 2018, doi: [10.1007/s00289-017-2090-3](https://doi.org/10.1007/s00289-017-2090-3).
- [154] W. Sun *et al.*, "The bioprinting roadmap," *Biofabrication*, vol. 12, no. 2, Feb. 2020, Art. no. 022002.
- [155] Y. Wu, Z. Y. Lin, A. C. Wenger, K. C. Tam, and X. Tang, "3D bioprinting of liver-mimetic construct with alginate/cellulose nanocrystal hybrid bioink," *Bioprinting*, vol. 9, pp. 1–6, 2018, doi: [10.1016/j.bprint.2017.12.001](https://doi.org/10.1016/j.bprint.2017.12.001).
- [156] R. Chang, K. Emami, H. Wu, and W. Sun, "Biofabrication of a three-dimensional liver micro-organ as an in vitro drug metabolism model," *Biofabrication*, vol. 2, no. 4, Dec. 2010, Art. no. 045004.
- [157] A. Faulkner-Jones *et al.*, "Bioprinting of human pluripotent stem cells and their directed differentiation into hepatocyte-like cells for the generation of mini-livers in 3D," *Biofabrication*, vol. 7, no. 4, Oct. 2015, Art. no. 044102.
- [158] M. Li, X. Tian, N. Zhu, D. J. Schreyer, and X. Chen, "Modeling process-induced cell damage in the bioprinting process," *Tissue Eng. Part C Methods*, vol. 16, no. 3, pp. 533–542, Jun. 2010.
- [159] D. G. Nguyen *et al.*, "Bioprinted 3D primary liver tissues allow assessment of organ-level response to clinical drug induced toxicity in vitro," *PLoS One*, vol. 11, no. 7, Jul. 2016, Art. no. e0158674.
- [160] H. Lee *et al.*, "Cell-printed 3D liver-on-a-chip possessing a liver microenvironment and biliary system," *Biofabrication*, vol. 11, no. 2, Jan. 2019, Art. no. 025001.
- [161] L. M. Norona, D. G. Nguyen, D. A. Gerber, S. C. Presnell, and E. L. LeCluyse, "Editor's highlight: Modeling compound-induced fibrogenesis in vitro using three-dimensional bioprinted human liver tissues," *Toxicol. Sci.*, vol. 154, no. 2, pp. 354–367, Dec. 2016.
- [162] S. Sharma, "Antituberculosis drugs and hepatotoxicity," *Infection, Genet. Evol.*, vol. 4, no. 2, pp. 167–170, 2004, doi: [10.1016/j.meegid.2003.01.001](https://doi.org/10.1016/j.meegid.2003.01.001).
- [163] S. Babai, L. Auclert, and H. Le-Louët, "Safety data and withdrawal of hepatotoxic drugs," *Therapie*, vol. 76, pp. 715–723, Feb. 2018, doi: [10.1016/j.therap.2018.02.004](https://doi.org/10.1016/j.therap.2018.02.004).
- [164] P. Datta, M. Dey, Z. Ataie, D. Unutmaz, and I. T. Ozbolat, "3D bioprinting for reconstituting the cancer microenvironment," *NPJ Precis. Oncol.*, vol. 4, no. 1, Jul. 2020, Art. no. 18.
- [165] Y. Kang, P. Datta, S. Shanmughapriya, and I. T. Ozbolat, "3D Bioprinting of tumor models for cancer research," *ACS Appl. Bio Mater.*, vol. 3, no. 9, pp. 5552–5573, 2020, doi: [10.1021/acsabm.0c00791](https://doi.org/10.1021/acsabm.0c00791).
- [166] H.-F. Tsai, A. Trubelja, A. Q. Shen, and G. Bao, "Tumour-on-a-chip: Microfluidic models of tumour morphology, growth and microenvironment," *J. R. Soc. Interface*, vol. 14, no. 131, Jun. 2017, Art. no. 20170137, doi: [10.1098/rsif.2017.0137](https://doi.org/10.1098/rsif.2017.0137).
- [167] M. A. Hermida *et al.*, "Three dimensional in vitro models of cancer: Bioprinting multilineage glioblastoma models," *Adv. Biol. Regulation*, vol. 75, Jan. 2020, Art. no. 100658.
- [168] M. A. Heinrich, R. Bansal, T. Lammers, Y. S. Zhang, R. M. Schifferers, and J. Prakash, "3D-Bioprinted Mini-Brain: A glioblastoma model to study cellular interactions and therapeutics," *Adv. Mater.*, vol. 31, no. 14, 2019, Art. no. 1806590, doi: [10.1002/adma.201806590](https://doi.org/10.1002/adma.201806590).
- [169] X. Wang *et al.*, "Coaxial extrusion bioprinted shell-core hydrogel microfibers mimic glioma microenvironment and enhance the drug resistance of cancer cells," *Colloids Surf. B Biointerfaces*, vol. 171, pp. 291–299, Nov. 2018.
- [170] H.-G. Yi *et al.*, "A bioprinted human-glioblastoma-on-a-chip for the identification of patient-specific responses to chemoradiotherapy," *Nature Biomed. Eng.*, vol. 3, no. 7, pp. 509–519, Jul. 2019.
- [171] F. Xie *et al.*, "Three-dimensional bio-printing of primary human hepatocellular carcinoma for personalized medicine," *Biomaterials*, vol. 265, Jan. 2021, Art. no. 120416.
- [172] L. Sun *et al.*, "Application of a 3D bioprinted hepatocellular carcinoma cell model in antitumor drug research," *Front. Oncol.*, vol. 10, Jun. 2020, Art. no. 878.
- [173] X. Wang *et al.*, "Tumor-like lung cancer model based on 3D bioprinting," *3 Biotech*, vol. 8, no. 12, Dec. 2018, Art. no. 501.

- [174] A. Mondal *et al.*, "Characterization and printability of sodium alginate-Gelatin hydrogel for bioprinting NSCLC co-culture," *Sci. Rep.*, vol. 9, no. 1, 2019, doi: [10.1038/s41598-019-55034-9](https://doi.org/10.1038/s41598-019-55034-9).
- [175] P. A. Mollica *et al.*, "3D bioprinted mammary organoids and tumoroids in human mammary derived ECM hydrogels," *Acta Biomater.*, vol. 95, pp. 201–213, Sep. 2019.
- [176] E. M. Langer *et al.*, "Modeling tumor phenotypes in vitro with three-dimensional bioprinting," *Cell Rep.*, vol. 26, no. 3, pp. 608–623.e6, 2019, doi: [10.1016/j.celrep.2018.12.090](https://doi.org/10.1016/j.celrep.2018.12.090).
- [177] D. Hakobyan *et al.*, "Laser-assisted 3D bioprinting of exocrine pancreas spheroid models for cancer initiation study," *Biofabrication*, vol. 12, no. 3, 2020, Art. no. 035001, doi: [10.1088/1758-5090/ab7cb8](https://doi.org/10.1088/1758-5090/ab7cb8).
- [178] F. Xu, J. Celli, I. Rizvi, S. Moon, T. Hasan, and U. Demirci, "A three-dimensional in vitro ovarian cancer coculture model using a high-throughput cell patterning platform," *Biotechnol. J.*, vol. 6, no. 2, pp. 204–212, Feb. 2011.
- [179] Y. Pang *et al.*, "TGF- β induced epithelial-mesenchymal transition in an advanced cervical tumor model by 3D printing," *Biofabrication*, vol. 10, no. 4, 2018, Art. no. 044102, doi: [10.1088/1758-5090/aadbde](https://doi.org/10.1088/1758-5090/aadbde).
- [180] Y. Zhao *et al.*, "Three-dimensional printing of hela cells for cervical tumor model in vitro," *Biofabrication*, vol. 6, no. 3, Sep. 2014, Art. no. 035001.
- [181] "The biology of personalized cancer medicine: Facing individual complexities underlying hallmark capabilities," *Mol. Oncol.*, vol. 6, no. 2, pp. 111–127, Apr. 2012.
- [182] M. Fung, A. Thornton, K. Mybeck, J. H.-H. Wu, K. Hornbuckle, and E. Muniz, "Evaluation of the characteristics of safety withdrawal of prescription drugs from Worldwide pharmaceutical markets-1960 to 1999," *Drug Inf. J.*, vol. 35, no. 1, pp. 293–317, 2001, doi: [10.1177/009286150103500134](https://doi.org/10.1177/009286150103500134).
- [183] N. Ferri, P. Siegl, A. Corsini, J. Herrmann, A. Lerman, and R. Benghozi, "Drug attrition during pre-clinical and clinical development: Understanding and managing drug-induced cardiotoxicity," *Pharmacol. Therapeutics*, vol. 138, no. 3, pp. 470–484, Jun. 2013.
- [184] X. Li, R. Zhang, B. Zhao, C. Lossin, and Z. Cao, "Cardiotoxicity screening: A review of rapid-throughput in vitro approaches," *Arch. Toxicol.*, vol. 90, no. 8, pp. 1803–1816, Aug. 2016.
- [185] A. Mazzocchi, S. Soker, and A. Skardal, "3D bioprinting for high-throughput screening: Drug screening, disease modeling, and precision medicine applications," *Appl. Phys. Rev.*, vol. 6, no. 1, Mar. 2019, Art. no. 011302, doi: [10.1063/1.5056188](https://doi.org/10.1063/1.5056188).
- [186] A. C. Daly, M. D. Davidson, and J. A. Burdick, "3D bioprinting of high cell-density heterogeneous tissue models through spheroid fusion within self-healing hydrogels," *Nature Commun.*, vol. 12, no. 1, Feb. 2021, Art. no. 753.
- [187] Y. S. Zhang *et al.*, "Bioprinting 3D microfibrous scaffolds for engineering endothelialized myocardium and heart-on-a-chip," *Biomaterials*, vol. 110, pp. 45–59, 2016, doi: [10.1016/j.biomaterials.2016.09.003](https://doi.org/10.1016/j.biomaterials.2016.09.003).
- [188] A. Kjar, B. McFarland, K. Mecham, N. Harward, and Y. Huang, "Engineering of tissue constructs using coaxial bioprinting," *Bioactive Mater.*, vol. 6, no. 2, pp. 460–471, Feb. 2021.
- [189] Q. Gao, Y. He, J.-Z. Fu, A. Liu, and L. Ma, "Coaxial nozzle-assisted 3D bioprinting with built-in microchannels for nutrients delivery," *Biomaterials*, vol. 61, pp. 203–215, Aug. 2015.
- [190] G. Gao, J. Y. Park, B. S. Kim, J. Jang, and D.-W. Cho, "Coaxial cell printing of freestanding, perfusable, and functional in vitro vascular models for recapitulation of native vascular endothelium pathophysiology," *Adv. Healthc. Mater.*, vol. 7, no. 23, Dec. 2018, Art. no. e1801102.
- [191] J. Schöneberg *et al.*, "Engineering biofunctional in vitro vessel models using a multilayer bioprinting technique," *Sci. Rep.*, vol. 8, no. 1, 2018, Art. no. 10430, doi: [10.1038/s41598-018-28715-0](https://doi.org/10.1038/s41598-018-28715-0).
- [192] F. M. Watt, "Mammalian skin cell biology: At the interface between laboratory and clinic," *Science*, vol. 346, no. 6212, pp. 937–940, 2014, doi: [10.1126/science.1253734](https://doi.org/10.1126/science.1253734).
- [193] V. Lee *et al.*, "Design and fabrication of human skin by three-dimensional bioprinting," *Tissue Eng. Part C: Methods*, vol. 20, no. 6, pp. 473–484, 2014, doi: [10.1089/ten.tec.2013.0335](https://doi.org/10.1089/ten.tec.2013.0335).
- [194] B. S. Kim *et al.*, "3D cell printing of in vitro stabilized skin model and in vivo pre-vascularized skin patch using tissue-specific extracellular matrix bioink: A step towards advanced skin tissue engineering," *Biomaterials*, vol. 168, pp. 38–53, Jun. 2018.
- [195] P. Admane *et al.*, "Direct 3D bioprinted full-thickness skin constructs recapitulate regulatory signaling pathways and physiology of human skin," *Bioprinting*, vol. 15, 2019, Art. no. e00051, doi: [10.1016/j.bprint.2019.e00051](https://doi.org/10.1016/j.bprint.2019.e00051).
- [196] L. Koch *et al.*, "Skin tissue generation by laser cell printing," *Biotechnol. Bioeng.*, vol. 109, no. 7, pp. 1855–1863, Jul. 2012.
- [197] L. J. Pourchet *et al.*, "Human skin 3D bioprinting using scaffold-free approach," *Adv. Healthc. Mater.*, vol. 6, Feb. 2017, Art. no. 4, doi: [10.1002/adhm.201601101](https://doi.org/10.1002/adhm.201601101).
- [198] Z. Wei *et al.*, "Two-Dimensional cellular and three-dimensional bioprinted skin models to screen topical-use compounds for irritation potential," *Front. Bioeng. Biotechnol.*, vol. 8, Feb. 2020, Art. no. 109.
- [199] V. Andre-Frei *et al.*, "Laser-Assisted bioprinted skin equivalent for cosmetic efficacy evaluation," in *Proc. 24th Int. Federation Societies Cosmetic Chemists*, Seoul, South Korea, Accessed: Nov. 2021. [Online]. Available: <https://www.axt.com.au/wp-content/uploads/Poietis-BASF-bioprinted-skin-model.pdf>
- [200] Y. Zhang *et al.*, "Using bioprinting and spheroid culture to create a skin model with sweat glands and hair follicles," *Burns Trauma*, vol. 9, 2021, Art. no. tkab013, doi: [10.1093/burnst/tkab013](https://doi.org/10.1093/burnst/tkab013).
- [201] W. L. Ng, J. T. Z. Qi, W. Y. Yeong, and M. W. Naing, "Proof-of-concept: 3D bioprinting of pigmented human skin constructs," *Biofabrication*, vol. 10, no. 2, Jan. 2018, Art. no. 025005.
- [202] D. Min, W. Lee, I.-H. Bae, T. R. Lee, P. Croce, and S.-S. Yoo, "Bioprinting of biomimetic skin containing melanocytes," *Exp. Dermatol.*, vol. 27, no. 5, pp. 453–459, May 2018.
- [203] R. A. Briggaman and C. E. Wheeler, Jr., "The epidermal-dermal junction," *J. Invest. Dermatol.*, vol. 65, no. 1, pp. 71–84, Jul. 1975.
- [204] R. E. Burgeson and A. M. Christiano, "The dermal—Epidermal junction," *Curr. Opin. Cell Biol.*, vol. 9, no. 5, pp. 651–658, Oct. 1997.
- [205] H. Yousef, J. H. Miao, M. Alhajj, and T. Badri, "Histology, skin appendages," in *StatPearls [Internet]*, Treasure Island, FL, USA: StatPearls Publishing, 2021, pp. 1–6.
- [206] J. C. Vary, "Selected disorders of skin appendages—Acne, alopecia, hyperhidrosis," *Med. Clin. North Amer.*, vol. 99, no. 6, pp. 1195–1211, 2015, doi: [10.1016/j.mcna.2015.07.003](https://doi.org/10.1016/j.mcna.2015.07.003).
- [207] A. Patzelt and J. Lademann, "The increasing importance of the hair follicle route in dermal and transdermal drug delivery," in *Percutaneous Penetration Enhancers Chemical Methods in Penetration Enhancement*. Berlin, Germany: Springer, 2015, pp. 43–53, doi: [10.1007/978-3-662-45013-0_5](https://doi.org/10.1007/978-3-662-45013-0_5).
- [208] S. K. Jain, A. Verma, A. Jain, and P. Hurkat, "Transfollicular drug delivery: Current perspectives," in *Research and Reports in Transdermal Drug Delivery*. Macclesfield, U.K.: Dovpress, 2016, p. 1, doi: [10.2147/rtrd.s75809](https://doi.org/10.2147/rtrd.s75809).
- [209] R. A. Swerlick, "The structure and function of the cutaneous vasculature," *J. Dermatol.*, vol. 24, no. 11, pp. 734–738, 1997, doi: [10.1111/j.1346-8138.1997.tb02527.x](https://doi.org/10.1111/j.1346-8138.1997.tb02527.x).
- [210] R. Huggenberger and M. Detmar, "The cutaneous vascular system in chronic skin inflammation," *J. Invest. Dermatol. Symp. Proc.*, vol. 15, no. 1, pp. 24–32, Dec. 2011.
- [211] X. Liu, S. Michael, K. Bharti, M. Ferrer, and M. J. Song, "A bio-fabricated vascularized skin model of atopic dermatitis for preclinical studies," *Biofabrication*, vol. 12, no. 3, 2020, Art. no. 035002, doi: [10.1088/1758-5090/ab76a1](https://doi.org/10.1088/1758-5090/ab76a1).
- [212] Y. Gilaberte, L. Prieto-Torres, I. Pastushenko, and Á. Juarranz, "Anatomy and function of the skin," *Nanoscience Dermatol.*, vol. 2016, pp. 1–14, 2016, doi: [10.1016/b978-0-12-802926-8.00001-x](https://doi.org/10.1016/b978-0-12-802926-8.00001-x).
- [213] M. Blüher, "Clinical relevance of adipokines," *Diabetes Metab. J.*, vol. 36, no. 5, 2012, Art. no. 317, doi: [10.4093/dmj.2012.36.5.317](https://doi.org/10.4093/dmj.2012.36.5.317).
- [214] B. S. Kim, G. Gao, J. Y. Kim, and D.-W. Cho, "3D Cell printing of perfusable vascularized human skin equivalent composed of epidermis, dermis, and hypodermis for better structural recapitulation of native skin," *Adv. Healthcare Mater.*, vol. 8, no. 7, Apr. 2019, Art. no. e1801019.
- [215] B. S. Kim, M. Ahn, W.-W. Cho, G. Gao, J. Jang, and D.-W. Cho, "Engineering of diseased human skin equivalent using 3D cell printing for representing pathophysiological hallmarks of type 2 diabetes in vitro," *Biomaterials*, vol. 272, 2021, Art. no. 120776, doi: [10.1016/j.biomaterials.2021.120776](https://doi.org/10.1016/j.biomaterials.2021.120776).
- [216] C. Wu, B. Wang, C. Zhang, R. A. Wysk, and Y.-W. Chen, "Bioprinting: An assessment based on manufacturing readiness levels," *Crit. Rev. Biotechnol.*, vol. 37, no. 3, pp. 333–354, 2017, doi: [10.3109/07388551.2016.1163321](https://doi.org/10.3109/07388551.2016.1163321).
- [217] P. F. Costa, "Translating biofabrication to the market," *Trends Biotechnol.*, vol. 37, no. 10, pp. 1032–1036, Oct. 2019.
- [218] D. R. Mertz, T. Ahmed, and S. Takayama, "Engineering cell heterogeneity into organs-on-a-chip," *Lab Chip*, vol. 18, no. 16, pp. 2378–2395, Aug. 2018.

- [219] C.-C. Hon, J. W. Shin, P. Carninci, and M. J. T. Stubbington, "The human cell atlas: Technical approaches and challenges," *Brief. Funct. Genomic.*, vol. 17, no. 4, pp. 283–294, 2018, doi: [10.1093/bfpg/ely029](https://doi.org/10.1093/bfpg/ely029).
- [220] C. A. Silva, C. J. Cortés-Rodríguez, J. Hazur, S. Reakasame, and A. R. Boccaccini, "Rational design of a triple-layered coaxial extruder system: In silico and in vitro evaluations directed towards optimizing cell viability," *Int. J. Bioprinting*, vol. 6, no. 4, 2020, Art. no. 282, doi: [10.18063/ijb.v6i4.282](https://doi.org/10.18063/ijb.v6i4.282).
- [221] J. He, J. Shao, X. Li, Q. Huang, and T. Xu, "Bioprinting of coaxial multicellular structures for a 3D co-culture model," *Bioprinting*, vol. 11, 2018, Art. no. e00036, doi: [10.1016/j.bprint.2018.e00036](https://doi.org/10.1016/j.bprint.2018.e00036).
- [222] L. Shao, Q. Gao, C. Xie, J. Fu, M. Xiang, and Y. He, "Directly coaxial 3D bioprinting of large-scale vascularized tissue constructs," *Biofabrication*, vol. 12, no. 3, 2020, Art. no. 035014, doi: [10.1088/1758-5090/ab7e76](https://doi.org/10.1088/1758-5090/ab7e76).
- [223] Y. Wu, Y. Zhang, Y. Yu, and I. T. Ozbolat, "3D Coaxial bioprinting of vasculature," *Methods Mol. Biol.*, vol. 2140, pp. 171–181, 2020.
- [224] X. Dai *et al.*, "Coaxial 3D bioprinting of self-assembled multicellular heterogeneous tumor fibers," *Sci. Rep.*, vol. 7, no. 1, May 2017, Art. no. 1457.
- [225] C. Chávez-Madero *et al.*, "Using chaotic advection for facile high-throughput fabrication of ordered multilayer micro- and nanostructures: Continuous chaotic printing," *Biofabrication*, vol. 12, no. 3, Jun. 2020, Art. no. 035023.
- [226] C. F. Ceballos-González *et al.*, "Micro-biogeography greatly matters for competition: Continuous chaotic bioprinting of spatially-controlled bacterial microcosms," Jul. 2020. Accessed: Feb. 8, 2022, doi: [10.1101/2020.07.12.199307](https://doi.org/10.1101/2020.07.12.199307).
- [227] K. S. Patel and A. Thavamani, "Physiology, peristalsis," in *StatPearls [Internet]*, Treasure Island, FL, USA: StatPearls Publishing, 2020.
- [228] Y.-C. Li, Y. S. Zhang, A. Akpek, S. R. Shin, and A. Khademhosseini, "4D bioprinting: The next-generation technology for biofabrication enabled by stimuli-responsive materials," *Biofabrication*, vol. 9, no. 1, 2016, Art. no. 012001, doi: [10.1088/1758-5090/9/1/012001](https://doi.org/10.1088/1758-5090/9/1/012001).
- [229] B. Gao, Q. Yang, X. Zhao, G. Jin, Y. Ma, and F. Xu, "4D Bioprinting for biomedical applications," *Trends Biotechnol.*, vol. 34, no. 9, pp. 746–756, 2016, doi: [10.1016/j.tibtech.2016.03.004](https://doi.org/10.1016/j.tibtech.2016.03.004).
- [230] M. Jamal *et al.*, "Bio-origami hydrogel scaffolds composed of photocrosslinked PEG bilayers," *Adv. Healthcare Mater.*, vol. 2, no. 8, pp. 1142–1150, Aug. 2013.
- [231] A. Gandhi, A. Paul, S. O. Sen, and K. K. Sen, "Studies on thermoresponsive polymers: Phase behaviour, drug delivery and biomedical applications," *Asian J. Pharmaceut. Sci.*, vol. 10, no. 2, pp. 99–107, 2015, doi: [10.1016/j.ajps.2014.08.010](https://doi.org/10.1016/j.ajps.2014.08.010).
- [232] C. Aronsson *et al.*, "Dynamic peptide-folding mediated biofunctionalization and modulation of hydrogels for 4D bioprinting," *Biofabrication*, vol. 12, no. 3, Jul. 2020, Art. no. 035031.
- [233] Z. Liu, J. Liu, X. Cui, X. Wang, L. Zhang, and P. Tang, "Recent advances on magnetic sensitive hydrogels in tissue engineering," *Front. Chem.*, vol. 8, Mar. 2020, Art. no. 124.
- [234] Y. Luo, X. Lin, B. Chen, and X. Wei, "Cell-laden four-dimensional bioprinting using near-infrared-triggered shape-morphing alginate/polydopamine bioinks," *Biofabrication*, vol. 11, no. 4, Sep. 2019, Art. no. 045019.
- [235] S. Miao *et al.*, "Stereolithographic 4D bioprinting of multiresponsive architectures for neural engineering," *Adv. Biosyst.*, vol. 2, no. 9, Sep. 2018, Art. no. 1800101, doi: [10.1002/adbi.201800101](https://doi.org/10.1002/adbi.201800101).
- [236] T. J. Hinton *et al.*, "Three-dimensional printing of complex biological structures by freeform reversible embedding of suspended hydrogels," *Sci. Adv.*, vol. 1, no. 9, Oct. 2015, Art. no. e1500758.
- [237] A. Lee *et al.*, "3D bioprinting of collagen to rebuild components of the human heart," *Science*, vol. 365, no. 6452, pp. 482–487, Aug. 2019.
- [238] A. Isaacson, S. Swioklo, and C. J. C., "3D bioprinting of a corneal stroma equivalent," *Exp. Eye Res.*, vol. 173, pp. 188–193, Aug. 2018.
- [239] C. D. Lindsay, J. G. Roth, B. L. LeSavage, and S. C. Heilshorn, "Bioprinting of stem cell expansion lattices," *Acta Biomater.*, vol. 95, pp. 225–235, Sep. 2019.
- [240] Y.-J. Choi *et al.*, "A 3D cell printed muscle construct with tissue-derived bioink for the treatment of volumetric muscle loss," *Biomaterials*, vol. 206, pp. 160–169, Jun. 2019.
- [241] Y. Lu, G. Mapili, G. Suhali, S. Chen, and K. Roy, "A digital micro-mirror device-based system for the microfabrication of complex, spatially patterned tissue engineering scaffolds," *J. Biomed. Mater. Res. Part A*, vol. 77A, no. 2, pp. 396–405, 2006, doi: [10.1002/jbm.a.30601](https://doi.org/10.1002/jbm.a.30601).
- [242] B. Grigoryan *et al.*, "Multivascular networks and functional intravascular topologies within biocompatible hydrogels," *Science*, vol. 364, no. 6439, pp. 458–464, May 2019.
- [243] J. Zhang, Q. Hu, S. Wang, J. Tao, and M. Gou, "Digital light processing-based Three-dimensional printing for medical applications," *Int. J. Bioprint*, vol. 6, no. 1, 2020, Art. no. 242.
- [244] A. Casey, M. Gargotti, F. Bonnier, and H. J. Byrne, "Chemotherapeutic efficiency of drugs in vitro: Comparison of doxorubicin exposure in 3D and 2D culture matrices," *Toxicol. Vitro*, vol. 33, pp. 99–104, Jun. 2016.
- [245] E. A. Brooks, S. Galarza, M. F. Gencoglu, R. C. Cornelison, J. M. Munson, and S. R. Peyton, "Applicability of drug response metrics for cancer studies using biomaterials," *Philos. Trans. R. Soc. Lond. B Biol. Sci.*, vol. 374, no. 1779, Aug. 2019, Art. no. 20180226.
- [246] F. Bonnier *et al.*, "Cell viability assessment using the alamar blue assay: A comparison of 2D and 3D cell culture models," *Toxicol. Vitro*, vol. 29, no. 1, pp. 124–131, 2015, doi: [10.1016/j.tiv.2014.09.014](https://doi.org/10.1016/j.tiv.2014.09.014).
- [247] F. Armutcu, "Organ crosstalk: The potent roles of inflammation and fibrotic changes in the course of organ interactions," *Inflammation Res.*, vol. 68, no. 10, pp. 825–839, 2019, doi: [10.1007/s00011-019-01271-7](https://doi.org/10.1007/s00011-019-01271-7).
- [248] J. Eckel, *The Cellular Secretome and Organ Crosstalk*. Amsterdam, Netherlands: Elsevier, 2018, pp. 69–70, doi: [10.1016/c2015-0-06271-2](https://doi.org/10.1016/c2015-0-06271-2).
- [249] N. S. Bhise *et al.*, "A liver-on-a-chip platform with bioprinted hepatic spheroids," *Biofabrication*, vol. 8, no. 1, Jan. 2016, Art. no. 014101.
- [250] A. Agarwal, J. A. Goss, A. Cho, M. L. McCain, and K. K. Parker, "Microfluidic heart on a chip for higher throughput pharmacological studies," *Lab Chip*, vol. 13, no. 18, pp. 3599–3608, Sep. 2013.
- [251] M. Wufuer *et al.*, "Skin-on-a-chip model simulating inflammation, edema and drug-based treatment," *Sci. Rep.*, vol. 6, Nov. 2016, Art. no. 37471.
- [252] D. Huh *et al.*, "A human disease model of drug toxicity-induced pulmonary edema in a Lung-on-a-Chip microdevice," *Sci. Transl. Med.*, vol. 4, no. 159, pp. 159ra147, Nov. 2012.
- [253] A. Skardal *et al.*, "Multi-tissue interactions in an integrated three-tissue organ-on-a-chip platform," *Sci. Rep.*, vol. 7, no. 1, 2017, Art. no. 8837, doi: [10.1038/s41598-017-08879-x](https://doi.org/10.1038/s41598-017-08879-x).
- [254] A. Shpichka *et al.*, "Engineering a model to study viral infections: Bioprinting, microfluidics, and organoids to defeat coronavirus disease 2019 (COVID-19)," *Int. J. Bioprinting*, vol. 6, no. 4, 2020, Art. no. 302, doi: [10.18063/ijb.v6i4.302](https://doi.org/10.18063/ijb.v6i4.302).
- [255] S. E. Park, "Epidemiology, virology, and clinical features of severe acute respiratory syndrome -coronavirus-2 (SARS-CoV-2; coronavirus disease-19)," *Clin. Exp. Pediatrics*, vol. 63, no. 4, pp. 119–124, 2020, doi: [10.3345/cep.2020.00493](https://doi.org/10.3345/cep.2020.00493).
- [256] A. Kabir *et al.*, "3D Bioprinting for fabrication of tissue models of COVID-19 infection," *Essays Biochem.*, vol. 65, no. 3, pp. 503–518, Aug. 2021.